CHAPTER 1

Essential Concepts in Imaging Musculoskeletal Trauma

Andrea Donovan
Department of Medical Imaging, Sunnybrook Health Sciences Centre, University of Toronto, Toronto, Canada

Introduction

Traumatic injuries to the musculoskeletal system are extremely common. These injuries are among the short list of medical disorders that may be completely resolved if recognized and appropriately treated. As radiologists, we have an important role in the diagnosis. In order to identify the abnormality and characterize it correctly, it is essential to be familiar with normal anatomy, protocols for imaging tests, patterns of injury, and implement an organized approach to image interpretation. The radiology report needs to be concise, yet include relevant information required for effective clinical management. It is important to be familiar with common fracture classification systems and understand how different grades of injury potentially affect treatment. Furthermore, it is important to be familiar with common treatment options for fracture and joint fixation, and be able to recognize potential complications on follow-up imaging.

Throughout this book, we emphasize the importance of an organized approach for the interpretation of imaging studies. This systematic approach includes assessment of the soft tissues, since an abnormality in the soft tissues can point to an abnormality in the adjacent joint or bone. In addition to a general approach, a checklist at specific anatomic sites is also needed to ensure that common sites of injury are evaluated for a fracture or dislocation. These specific sites of injury are discussed in the subsequent chapters, including the spine, pelvis, major joints, and long bones.

Fracture mechanism and epidemiology

Traumatic injury to the skeletal system is common at all ages. The location and appearance of the fracture depends on the mechanism of injury, age of the patient, and predisposing factors, such as an underlying osseous lesion [1]. The most common mechanism of fractures in the adolescent population is sports-related [2]. Adults are more likely to sustain an injury related to their occupation or related to a motor vehicle accident. There is a significant difference in fracture incidence between adult males and females. Fractures are more common in men before the age of 50, while after the age 50, women experience more fractures due to osteoporosis [3]. In the elderly, routine daily activities may result in a fracture, such as walking or using the stairs [4].

Motor vehicle accidents are currently the leading cause of death between the ages of 5 and 34 years [5]. Injury in these patients is usually more extensive and severe, with involvement of the pelvis, the spine, several joints and long bones. Falls are a common mechanism of injury at any age. Falls from a height are usually related to occupation, such as construction work, and often result in multiple fractures [6]. A fall on the outstretched hand is a common mechanism and results in different fractures depending on patient age. Supracondylar distal humerus or distal radius metaphyseal fractures are common in children. Colles' type distal radius fractures predominate in adults and proximal humeral fractures are common in elderly females.

Fractures may result from either a direct force or an indirect force transmitted from a different site, away from the actual fracture. Radiographs are helpful to infer the mechanism of a fracture including the direction and magnitude of applied force [5–7].

Direct force

Direct forces on a bone include direct blow, crush injury, gunshot injury or sharp object laceration. Direct blows most commonly affect the forearm or leg. These may

Imaging Musculoskeletal Trauma: Interpretation and Reporting, First Edition. Edited by Andrea Donovan and Mark Schweitzer.

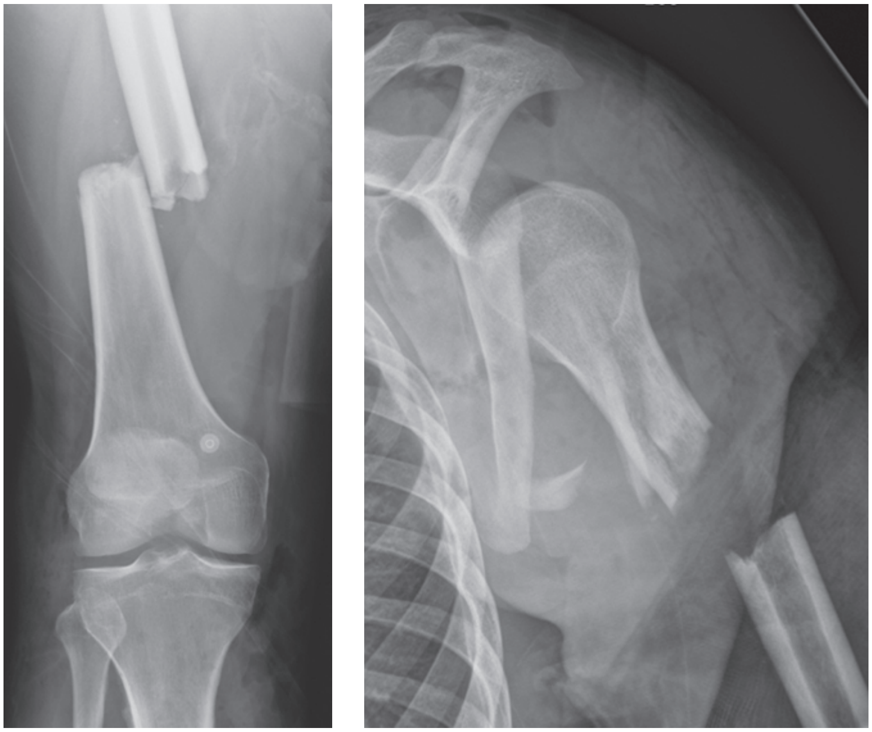

(a) (b)

Figure 1.1 Direct force resulting in transverse fractures. (a) High-velocity injury with transverse distal femoral shaft fracture with one shaft-width lateral displacement and mild overlap.
(b) High-energy crush injury to the arm with a large soft tissue defect in the proximal arm and predominantly transverse, fragmented, distracted proximal humerus shaft fracture.

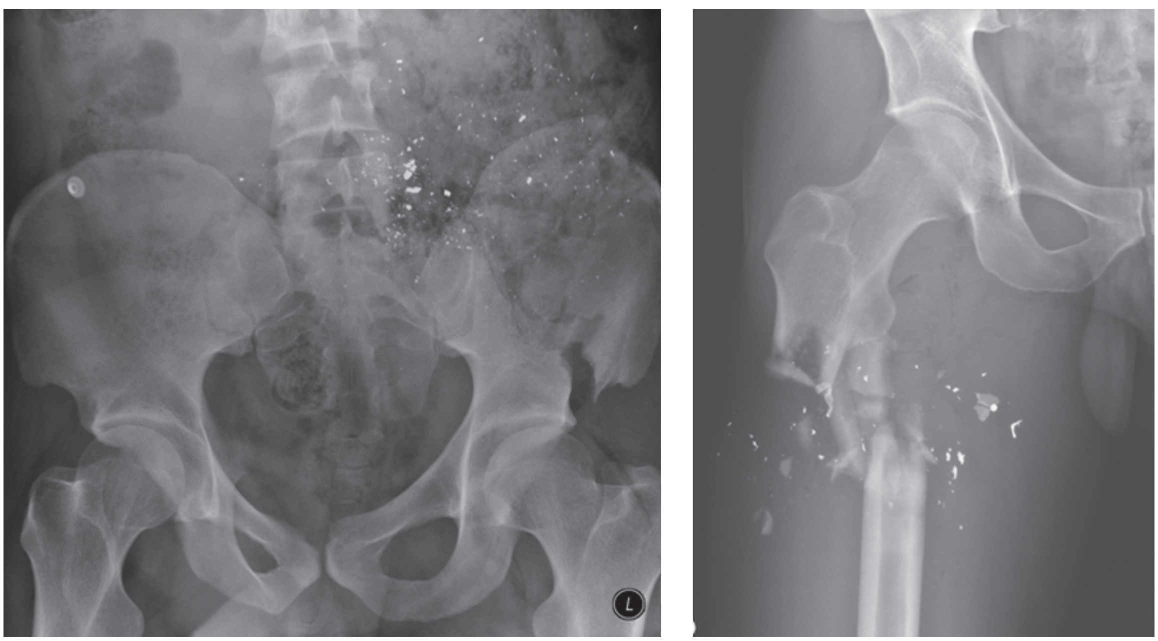

(a) (b)

Figure 1.2 Gunshot injuries and open fractures. (a) Pelvis radiograph shows radiodense bullet fragments projecting over the left lower quadrant with an associated comminuted iliac fracture. Mottled lucency represents soft tissue gas. (b) Hip radiograph in a different patient shows multiple metallic fragments in the soft tissues of the thigh and a comminuted proximal femoral shaft fracture. Soft tissue gas is seen about the fracture.

result in a transverse fracture to the ulna (nightstick fracture), or a transverse fracture to the tibia or the femur (Figure 1.1(a)). High-energy crush injury results in fragmentation of bone and there is usually a component of soft tissue injury (Figure 1.1(b)). Gunshot related fractures either result in severe comminution in cases of high-velocity bullet injury, or a divot in the cortex in cases of low-velocity ballistic injury (Figure 1.2). Saw injury is common in metal sheet workers and may result in a complete or incomplete traumatic amputations or lacerations, usually of the hand (Figure 1.3).

Figure 1.3 Crush injury with soft tissue amputation and associated fractures to the tufts of the index and long fingers.

Indirect force

Indirect forces on a bone include compression, tension, shear, rotation, and bending forces. Fractures may result from only one of these vectors, or more commonly, a combination of vectors. The resultant fracture orientation on radiographs can be used to infer the original dominant force vector.

Compression force compacts or pushes two objects together. It results in an oblique fracture of a long bone (Figure 1.4). Examples include fracture of the distal fibula with ankle inversion injury and resultant compression laterally. Compression is rarely the only force acting on a long bone. There is usually a combination of compression and angulation forces that lead to a shearing vector. Compression force is a frequent vector in spine injuries.

Shear force slides two parts of an object in opposite direction past one another. It results in an oblique fracture of a long bone. These fractures tend to be less stable than others. There is also often a compression vector involved that is present in addition to the shear vector (Figure 1.4(b)).

Tension force pulls or stretches two objects apart. It results in a transverse fracture. Examples include medial malleolar fracture following ankle eversion (Figure 1.5), olecranon fracture from pull of the triceps tendon or patella fracture related to pull of the quadriceps tendon.

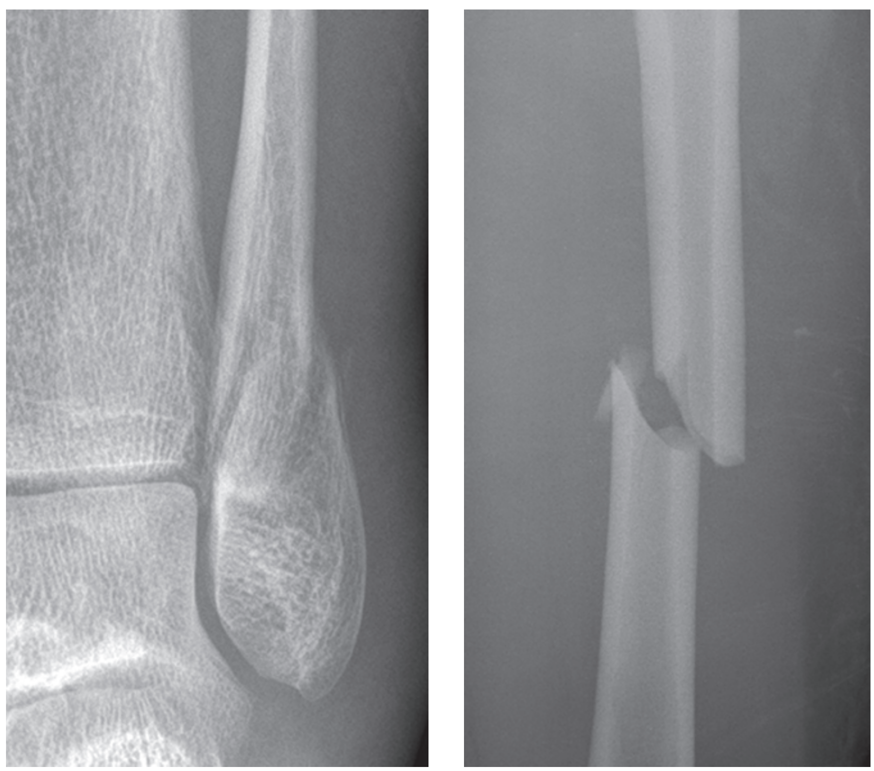

(a) (b)

Figure 1.4 Compression and shear forces resulting in oblique fractures. (a) Oblique distal fibular fracture related to a combination of compression and angulation. (b) Oblique midshaft femur fracture related to compression and shear vector.

Rotation force twists an object. It results in a spiral fracture, most commonly seen in the leg (Figure 1.5). Spiral fracture may be distinguished from an oblique fracture by the presence of two fracture planes.

Figure 1.5 Tension and rotation force resulting in transverse and spiral fractures. AP view of the ankle shows a transverse medial malleolar fracture related to avulsion by an intact deltoid ligament. Spiral fibular fracture shows two distinct fracture planes (arrows).

Bending or angulation force produces a curve on an object with resultant tension vector on the convex side and compression vector on the concave side. These fractures tend to produce a butterfly fragment along the concave, compression side (Figure 1.6).

Appropriateness criteria for imaging musculoskeletal trauma

The American College of Radiology (ACR) devised several guidelines for selecting the appropriate imaging test in a patient who sustained musculoskeletal trauma. These guidelines are published as ACR Appropriateness Criteria® for several clinical scenarios including suspected spine trauma, acute shoulder pain, acute trauma to the hand and wrist, to the knee, and to the foot and ankle. These guidelines are available on the ACR web site (www.acr.org/ac). In addition, there are several clinical guidelines that help clinicians select patients who do, or do not, require radiographs to evaluate their injury. These clinical guidelines include the Ottawa Ankle Rules [8], the Ottawa Knee Rule [9], and the Canadian Cervical Spine Rule [10].

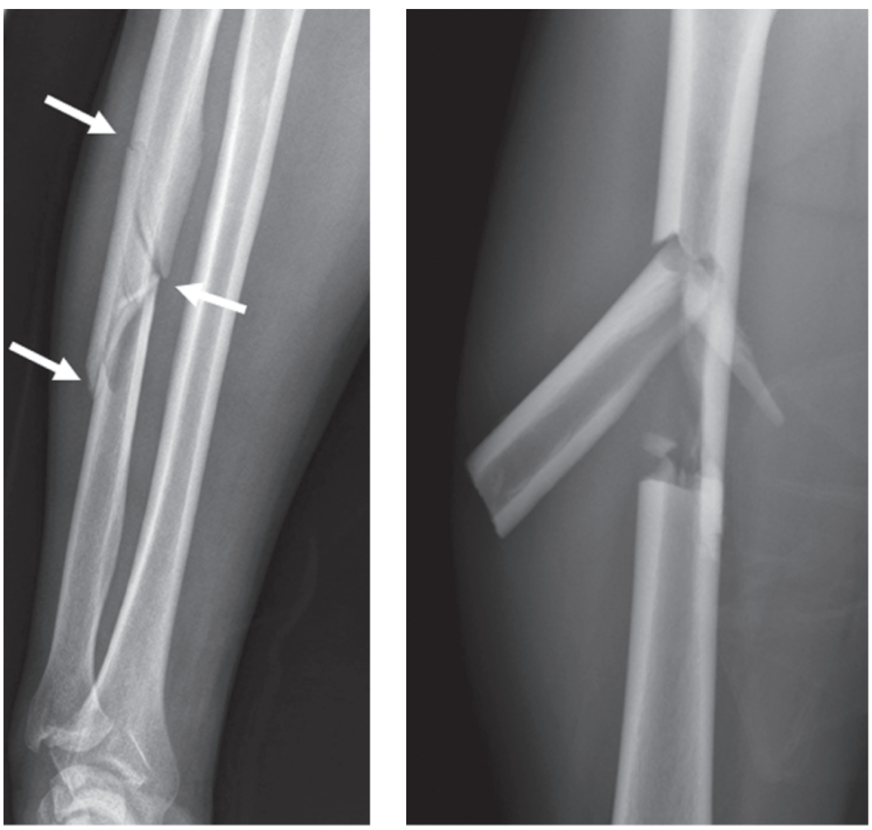

(a) (b)

Figure 1.6 Bending and angulation force resulting in a butterfly fragment. (a) Butterfly fragment along the mid-ulnar shaft (arrows). (b) Displaced butterfly fragment in a mid-femoral bending wedge fracture. Bending force results in a tension vector on the convex side and compression vector on the concave side. Butterfly fragment is seen on the concave, compression side.

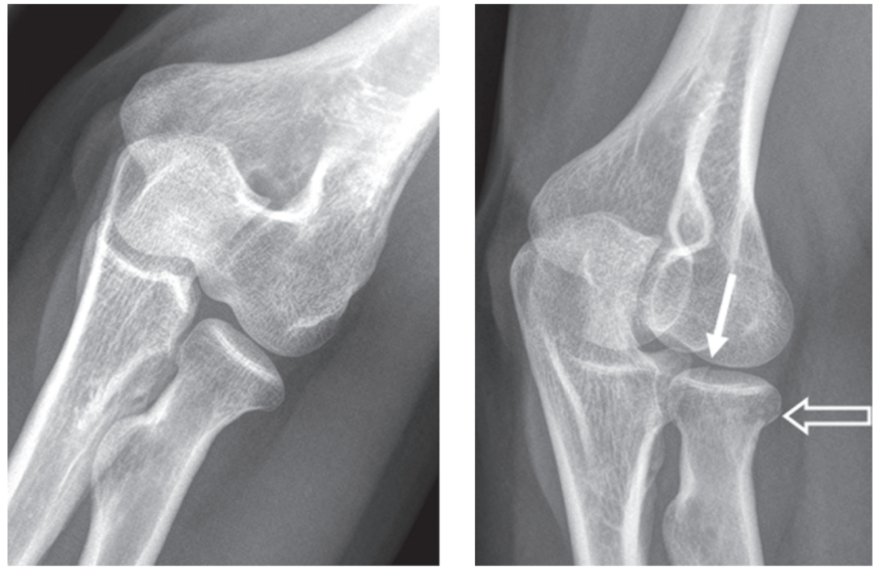

Figure 1.7 Importance of oblique views for fracture detection. (a) AP view does not show a definite radial head fracture. (b) Oblique view clearly demonstrates a fracture lucency (open arrow) and extension to the articular surface (closed arrow).

Radiographs

Radiographs are the initial imaging test of choice following skeletal trauma. The decision to perform a radiograph usually depends on the clinical history and physical examination. There may be, however, additional influencing factors such as patient expectations and fear of litigation. It is therefore important to be familiar with the indications for imaging in order to limit unnecessary exams. Up to 75% of skeletal radiographs in the emergency room are normal, with the greatest proportion of these being cervical spine and knee radiographs [11].

Most fractures can be detected on standard trauma series radiographs. In situations where there is a high clinical suspicion for a fracture, but negative radiographs, the patient may be splinted and repeat radiographs performed in 6 to 10 days. This may help to identify a somewhat more overt, subacute fracture.

In the polytrauma patient, it may not be possible to obtain adequate views. In that setting, cross sectional imaging with computed tomography (CT) is recommended. CT is also recommended in complex fractures at a joint, pelvic fractures and spine injury. Magnetic Resonance (MR) imaging is occasionally helpful in cases of occult fractures, or when there is concern for associated ligament or articular cartilage injury. Ultrasound is used in the assessment of soft tissue injury, and most commonly in the setting of tendon tears such as the quadriceps or the Achilles. Most foreign bodies can also be well visualized on ultrasound.

Radiographs should be obtained in a minimum of two orthogonal projections. Additional oblique or axial views are often useful to accurately detect a fracture. For example, tibial plateau fractures and radial head fractures may only be seen on the oblique view (Figure 1.7), while the axillary view of the shoulder is often needed to evaluate for shoulder articular congruence. Special views are described in subsequent chapters for each anatomic site. Stress-views are obtained with application of manual stress, and help in detection of ligament injury at the ankle (Figure 1.8), wrist or the knee for example. These are rarely useful in the acute setting, because soft tissue swelling and muscle spasm may mask underlying ligament injury [12].

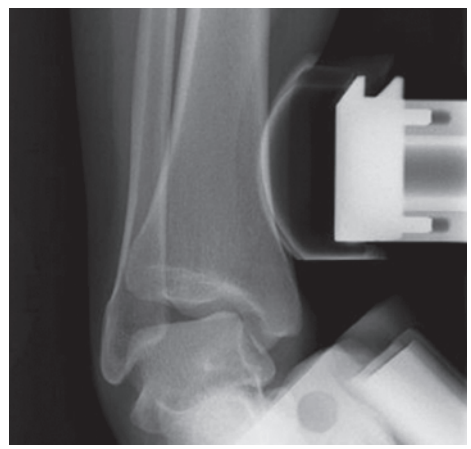

Figure 1.8 Stress view to evaluate ligament insufficiency at the ankle. Telos ankle apparatus is shown with varus stress applied to the ankle. There is abnormal widening of the lateral ankle gutter, which was absent on the nonstress views.

Computed Tomography (CT)

CT is commonly used in the trauma patient to identify and characterize the injury. The advantage of CT over radiography is the ability to identify subtle fractures, visualize articular fracture extension and assess for the presence of articular step-off or gap. Small intra-articular bodies that may prevent adequate reduction can also be visualized (Figure 1.9). Avulsion fractures on CT infer the presence of associated ligament or tendon injury. CT is also used to characterize fractures at complex anatomic sites such as the spine, pelvis, shoulder, elbow, sternoclavicular joint, and foot and ankle. At these locations, the overlap of osseous structures limits the ability of radiographs to accurately detect and characterize fractures [13].

Reformatted images in coronal and sagittal planes offer enhanced fracture detection. For example, axially oriented sacral fractures may only be detected on reformatted sagittal or coronal images, and not the axial images. Orthopedic surgeons find 3D reconstructed CT images helpful to visualize the position of fracture fragments and to plan the surgical approach (Figure 1.10). Most surgeons have a preference for translucent bone rendered images (Figure 1.10(a)) to show fracture relationships rather than surface rendered images (Figure 1.10(b)) that may partly obscure osseous detail. The addition of intravenous contrast facilitates evaluation for vascular injury including vasospasm, vessel transection, intimal injury and active extravasation (Figure 1.11). In many patients, CT angiography precludes the need for conventional angiography. Following reduction of a dislocation, CT is helpful to assess the adequacy of joint alignment and the congruency of articular surfaces. This congruence is especially important to prevent future osteoarthrosis. In patients with suspected delayed union or nonunion, CT can assess fracture healing, which is evident by osseous bridging.

Figure 1.9 CT for detection of intra-articular bodies. Sagittal reformatted image through the olecranon shows an intra-articular ossific body (arrow) within the joint in a patient who sustained an elbow fracture-dislocation.

Magnetic Resonance (MR) imaging

MR imaging is the modality of choice in the assessment of internal derangement of joints. This includes evaluation of the articular cartilage, ligaments, tendons, menisci, and fibrocartilagenous labrum. Occult fractures are also well visualized because of sensitivity of MR for marrow edema. Fracture lines are usually best depicted on T1-weighted sequences as linear low signal intensity. Surrounding marrow edema on T2-weighted sequences also helps to identify the fracture site. Subtle tibial plateau fractures, proximal or distal femur fractures may be radiographically occult, yet readily identified on MR (Figure 1.12) [14]. Bone bruises appear as an area of T2 hyperintense signal, with no discrete low signal intensity fracture line. Stress fractures in the long bone are characterized by a low signal intensity line on T1-weighted images with sur-

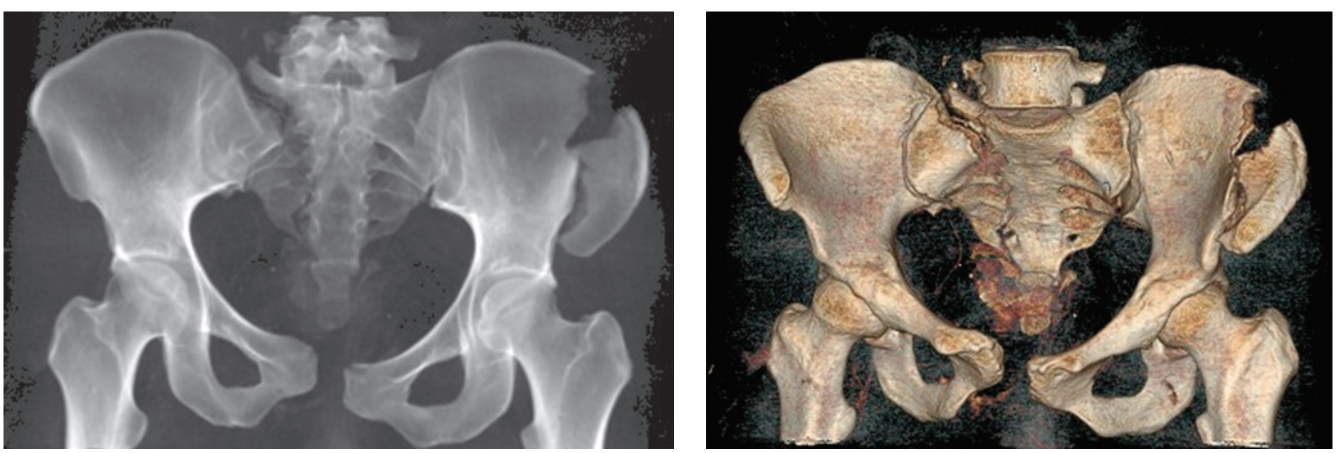

(a) (b)

Figure 1.10 Bone CT 3D reconstructed images. (a) Translucent bone 3D volume-rendered CT of AP pelvis and (b) bone 3D surface rendered images through the pelvis. Many orthopedic surgeons find these images helpful in planning surgery. This patient has a vertical shear injury with a distracted right sacral fracture, offset at the symphysis and left iliac wing distracted fracture. Translucent bone rendering in image (a) more clearly shows the fracture extent and relationships between fragments. Surface rendering in image (b) partly obscures the fracture by the overlying bone.

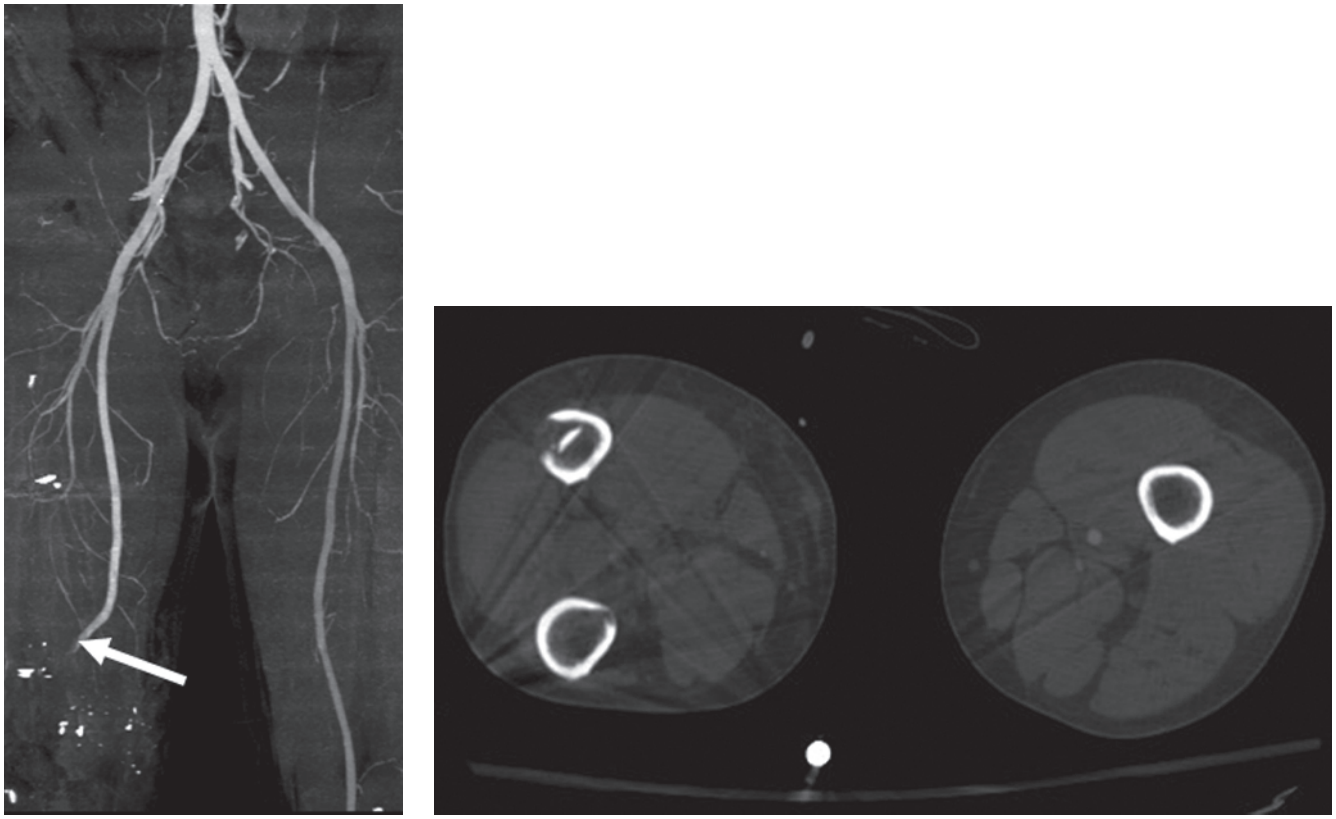

(a) (b)

Figure 1.11 CT angiogram in a patient with distal femoral displaced fracture. (a) Maximum intensity projection (MIP) image shows transection of the right popliteal artery (arrow). (b) Axial image shows a severely displaced right distal femoral shaft fracture with both the proximal and distal shaft visualized on the same image.

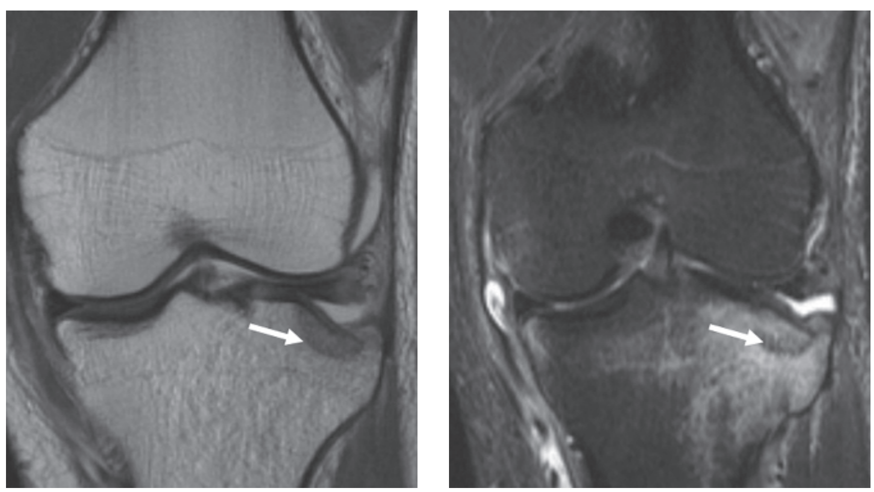

(a) (b)

Figure 1.12 Occult tibial plateau fracture on MR. (a) Coronal T1- and (b) T2-weighted, fat-suppressed images through the knee show a minimally depressed lateral tibial plateau fracture, with a low signal intensity fracture line paralleling the articular surface (arrow) and adjacent marrow edema. The fracture was not detected radiographically.

rounding marrow edema on T2-weighted images. In the midfoot, diffuse marrow edema, even in the absence of a discrete fracture line, may represent a fracture. Proton density sequence is reserved for imaging the menisci, articular cartilage, ligaments, and tendons (Figure 1.13(a)).

MR imaging of osteochondral injury is helpful to characterize the fragment size and potential stability [15–17]. Osteochondral fractures may be described as either displaced (fragment is at least partly displaced into the joint) or impacted (subchondral bone and overlying

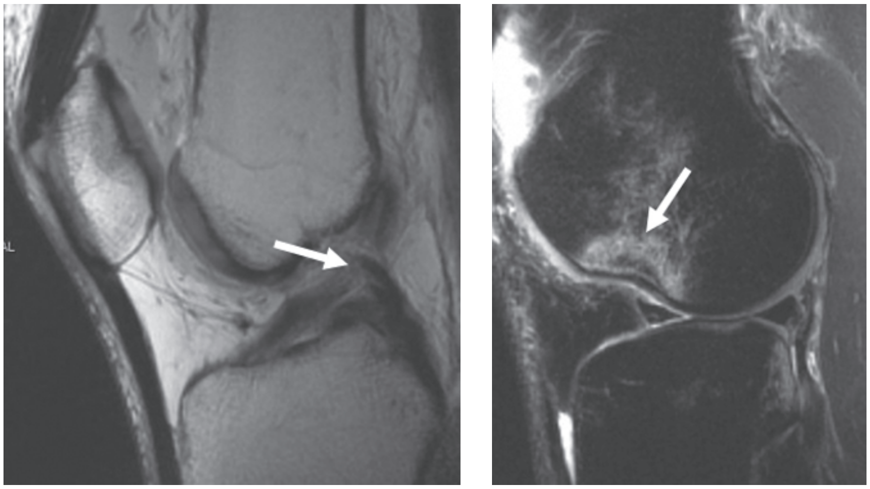

(a) (b)

Figure 1.13 Anterior cruciate ligament injury and femoral condyle osteochondral impaction injury. (a) Sagittal proton density image shows a discontinuity in the mid ACL fibers (arrow). (b) Sagittal T2-weighted fat-suppressed image shows an impacted fracture at the level of the lateral sulcus (arrow).

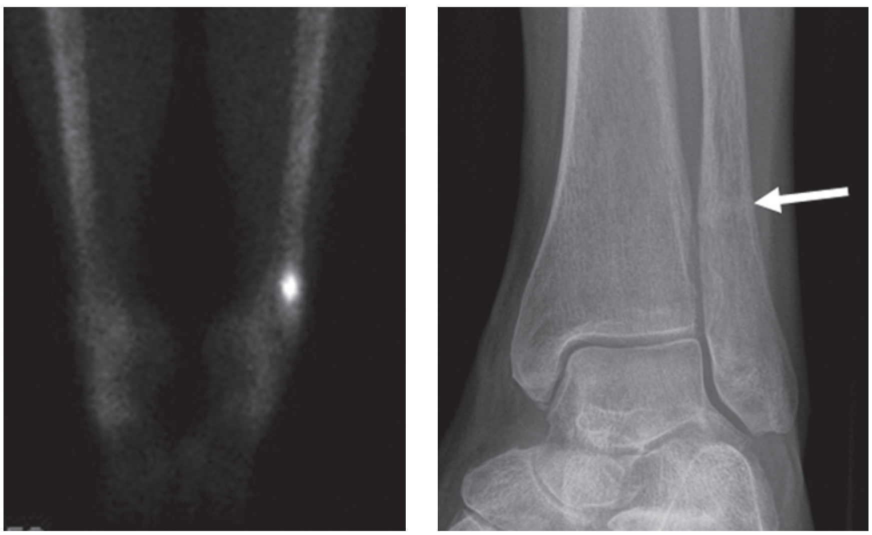

(a) (b)

Figure 1.14 Bone scan in an insufficiency fracture. (a) Static image from the bone scan shows focal increased activity in the left distal fibula. (b) Radiograph confirms the fracture evident by linear sclerosis in the distal fibular shaft (arrow).

cartilage are impacted into the adjacent medullary cavity with no major displaced osteochondral fragment) [15]. Typical displaced fractures include those of the patella following a dislocation, while typical impacted fractures include femoral condyle subchondral fractures (Figure 1.13(b)). MR is sensitive in the detection of displaced fragments into the joint. Impacted fractures are associated with extensive marrow edema on T2-weighted images. The typical appearance of a femoral condyle osteochondral impacted fracture is marrow edema extending all the way to the intercondylar notch and a low signal intensity line at the impaction site, paralleling the articular surface.

Bone scintigraphy

The most common use of bone scintigraphy in the setting of trauma is to facilitate detection of radiographically occult fractures, stress fractures and insufficiency fractures [18]. Bone scans are also used in situations where cross-sectional imaging is not available or is contraindicated. Specific clinical situations where bone scintigraphy is useful are fractures at the hip, scaphoid and some types of stress fractures [19]. The scintigraphic pattern varies with the age of the fracture, as well as the age of the patient. Approximately 80% of scans are positive within 24 hours of injury and 95% of scans are positive within 72 hours [20]. There are however, false negative scans, especially when evaluating acute injuries in elderly patients [21].

There are three characteristic scintigraphic patterns that reflect different stages of fracture healing [20]. The acute fracture appears as a diffuse area of increased activity at the fracture site, and this appearance will persist for 2 to 4 weeks after injury (Figure 1.14). The subacute fracture is characterized by a linear area of increased activity, and persists for 8 to 12 weeks. With further healing, the area of increased activity on bone scintigraphy gradually diminishes, but can persist for 5 to 7 months. In the vast

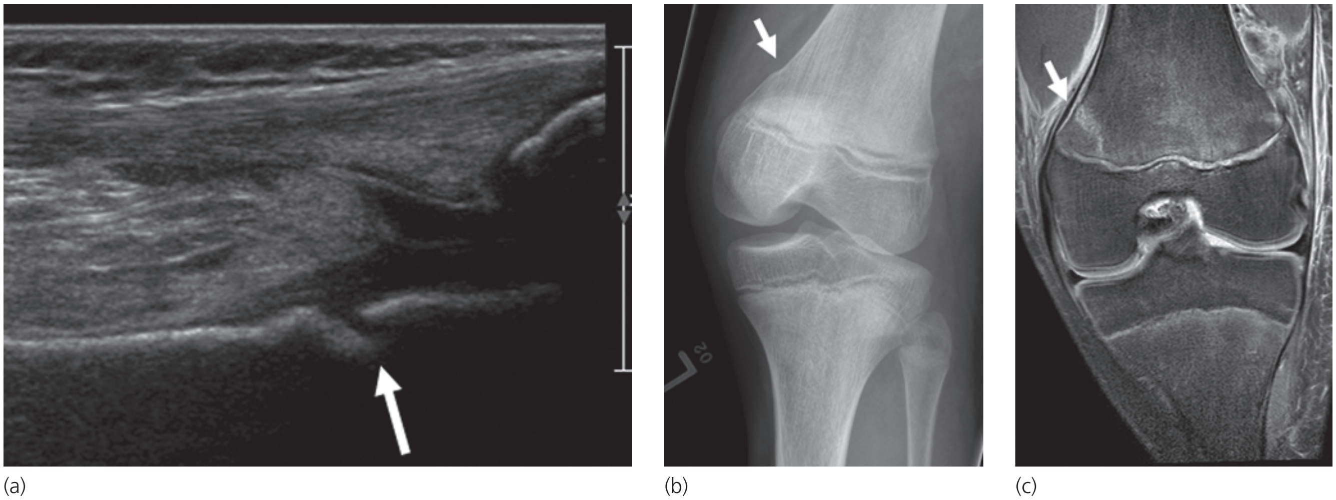

Figure 1.15 Ultrasound-detected fracture. (a) Sagittal image through the distal thigh shows a fracture (arrow) involving the distal demur, proximal to the patellofemoral joint. (b) AP radiograph confirms the fracture evident by cortical buckling (arrow). (c) Coronal fat-suppressed proton density image shows the bright fracture line and adjacent periosteal edema (arrow).

majority of patients (90%), the bone scan returns to normal within 2 years following injury [20]. In general, bone scans return to normal faster in younger patients.

Stress fractures can usually be identified on scintigraphy within 1 to 3 days of occurrence, while radiographs may remain negative for 2 to 3 weeks [22]. There are several mimickers of fractures on bone scintigraphy including metastatic disease, infection and traumatic synovitis [19].

Ultrasound

The primary role of ultrasound in the setting of trauma is the assessment of soft tissues. Ultrasound is useful in the characterization of focal tendon tears. The most common requests from the emergency department for musculoskeletal ultrasound include evaluation of the Achilles tendon, quadriceps tendon, distal insertion of the long head of biceps tendon and assessment of the rotator cuff [23, 24]. The presence of a complex joint effusion in the setting of trauma is compatible with a hemarthrosis and implies either a ligament injury or an intra-articular fracture. In patients who have sustained trauma, and have focal tenderness, it is important to evaluate the underlying cortex for a fracture. It is not infrequent that a fracture is detected on ultrasound when soft tissue injury is suspected clinically (Figure 1.15). Ultrasound can detect callus at an early stage of bone healing, and may have some role in fracture detection in infants [25].

Approach to accurate fracture detection on radiographs

Potential fracture mimickers

There are several potential mimickers of a fracture on radiographs. It is important to be familiar with the typical location and appearance of these mimickers to avoid mistaking them for a fracture. These potential mimickers include vascular channels, physeal fusion lines, and accessory ossicles. Visual misperception can also lead to the false positive interpretation of radiographs.

Vascular channels

Vascular channels for nutrient arteries are differentiated from fractures by sclerotic margins and their typical location and course. Vascular channels begin, and are more often seen, at the mid aspect of a long bone. A general rule is that vascular channels course diagonally so that they point toward the knee (Figure 1.16(a)), away from the elbow and toward the distal aspect of the phalanges [5]. Vascular channels should not extend into the medullary canal or involve any portion of the cortex that is not projected in profile.

Junctional lines

The junctional lines of fusion between the epiphysis and diaphysis, or the physeal scar, are most prominent in the lower extremities. These appear as a transverse sclerotic line in the metaphysis (Figure 1.16(b)). The location of junctional lines is predictable and should not be mistaken for an insufficiency or stress fracture. In the distal radius, the healed physis may mimic an intra-articular fracture.

Accessory ossicles

There are many accessory ossicles, some of which may be mistaken for a fracture, especially around the foot. These include an accessory navicular (Figure 1.16(c)) and the os peroneum. Accessory ossicles should be distinguished from a fracture based on sclerotic margins, rounded morphology, and typical locations. It is

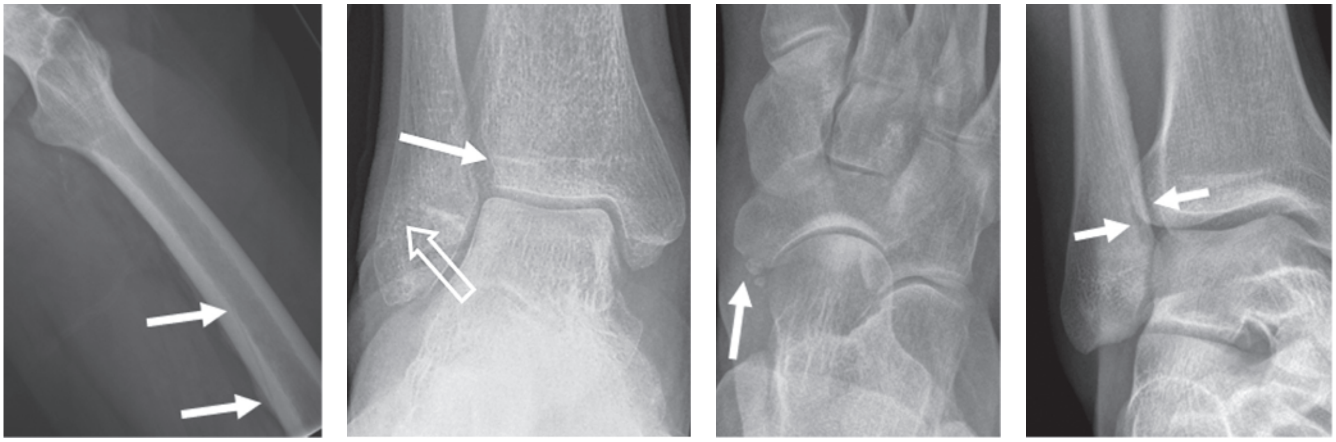

(a) (b) (c) (d)

Figure 1.16 Radiographic mimickers of fractures. (a) Vascular channel is shown in the distal femoral shaft (arrows). The margins are smooth and lucency is limited to the cortex. (b) Junctional line or physeal scar in the distal tibia (arrow) as well as a healing, lucent and sclerotic distal fibular fracture (open arrow). (c) Accessory navicular ossicles are well corticated (arrow). (d) Mach bands may simulate a fracture. They appear as lucent lines in the cortex of the tibia and fibula (arrows).

helpful to refer to the atlas of normal variants in cases of uncommon ossicles to verify that they indeed represent a normal variant.

Mach bands

Mach bands represent an optical illusion and should not be mistaken for a fracture. They appear at sites of cortex overlap between two bones, or skin fold overlap of the cortex [26]. This phenomenon is related in part to edge enhancement that the eye creates at the border between two superimposed objects. The mach bands appear as a lucent line and may be mistaken for a fracture. The most common site for this phenomenon is on ankle radiographs, where the tibia overlaps the fibula (Figure 1.16(d)).

Pattern search approach to radiographs in musculoskeletal trauma

1. Collect clinical information

In the trauma patient, it is important to collect information about the site and mechanism of injury prior to radiographic assessment. For multi-trauma patients, it is useful to know the most significant injury by reviewing additional imaging and reports. This information will help to guide search pattern for additional injuries that may occur with similar mechanisms. For example, a patient with a known calcaneal fracture should be carefully assessed for thoracolumbar spine burst fractures.

2. Compare to prior imaging

Prior imaging is sometimes available from an outside institution, and it is important to retrieve and review such imaging, if at all possible. A joint that appears reduced on the current study may have been dislocated on the prior study. This information is useful to guide the radiologist to inspect for fractures commonly associated with dislocations. If possible, the radiologist should obtain clinical history regarding the site of pain or the technologist can be advised to place markers at the site of tenderness [27]. This practice can improve fracture detection, especially in small bones.

3. Evaluate for radiographic signs of a fracture

Lucent fracture line

Most fractures appear as a radiolucent line. In nondisplaced fractures, the lucent line is thin and may be difficult to appreciate. In displaced fractures, with separation of fracture fragments, the fracture line is more overt (Figure 1.17). Visualization of the fracture on radiographs depends on the angle the X-ray beam makes with the fracture. Therefore, two orthogonal projections facilitate fracture detection. In 5% of fractures, the fracture line is only visualized on one of the two orthogonal projections. In another 5% of fractures, they are only visualized on an oblique (non-AP or lateral) projection. This is more common with fractures that occur at the end of the bone rather than involve the shaft (Figure 1.18). The vast majority of fractures however, are visualized in both AP and lateral projection.

Sclerotic fracture line

Compression fractures may appear as a sclerotic, rather than lucent line. The most common locations for traumatic compression are the vertebral bodies and distal radius related to axial loading (Figure 1.19(a)). A tibial

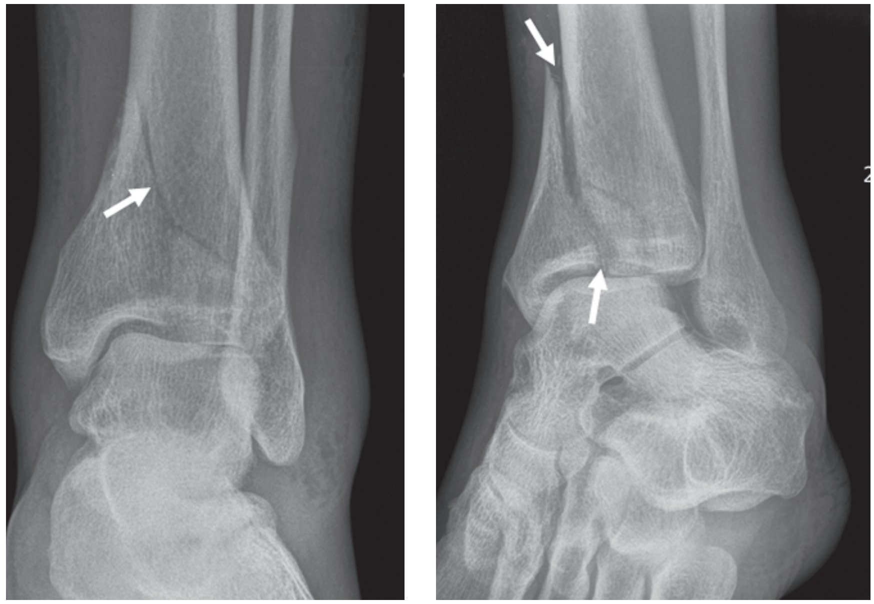

(a) (b)

Figure 1.17 Separation of fracture fragments. (a) AP view shows a faint lucent line in the distal tibia (arrow). (b) Oblique view shows separation of the fracture fragments and intra-articular extension (arrows).

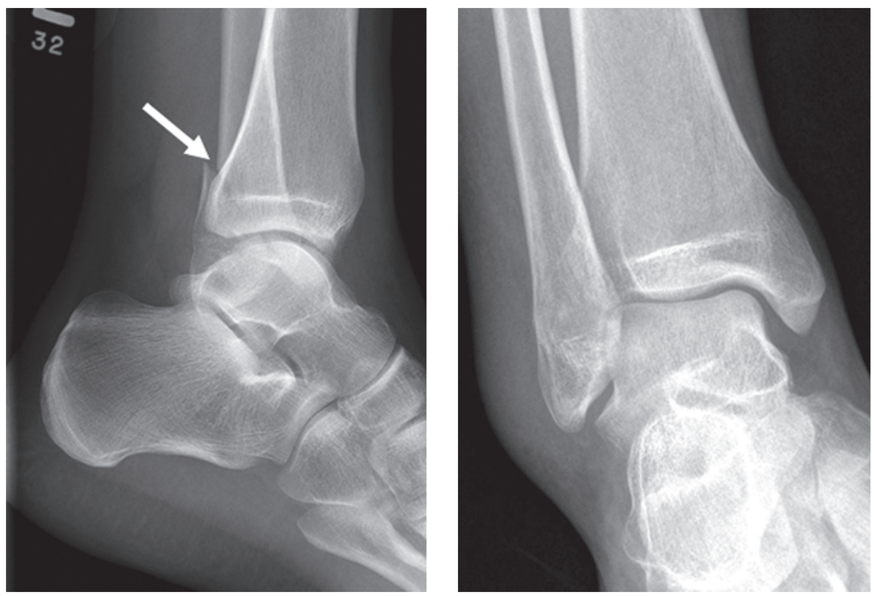

(a) (b)

Figure 1.18 Fibular fracture visible on lateral view only. (a) Lateral view of the ankle shows an oblique distal fibular fracture (arrow). (b) AP view shows lateral soft tissue swelling, but the fracture is not well visualized.

plateau depression fracture also often results in a sclerotic, rather than lucent fracture line.

Double line

Impaction fractures of a round end of the bone may appear as a sclerotic linear density or as a double line. Examples include a humeral head impacted fracture following a shoulder dislocation or a femoral head fracture following a hip dislocation (Figure 1.19(b)). The fracture is a result of impaction of a round articular surface against a firm edge of the adjacent bone. The result is a trough-like depression in the humeral or femoral head.

Cortical buckling

Commonly missed fractures are those that appear as cortical buckling in the absence of a fracture line traversing the bone. These can be seen in the distal radius and involving the radial neck region (Figure 1.20). Cortical buckling may only be seen on one view, so it is important to carefully inspect all projections.

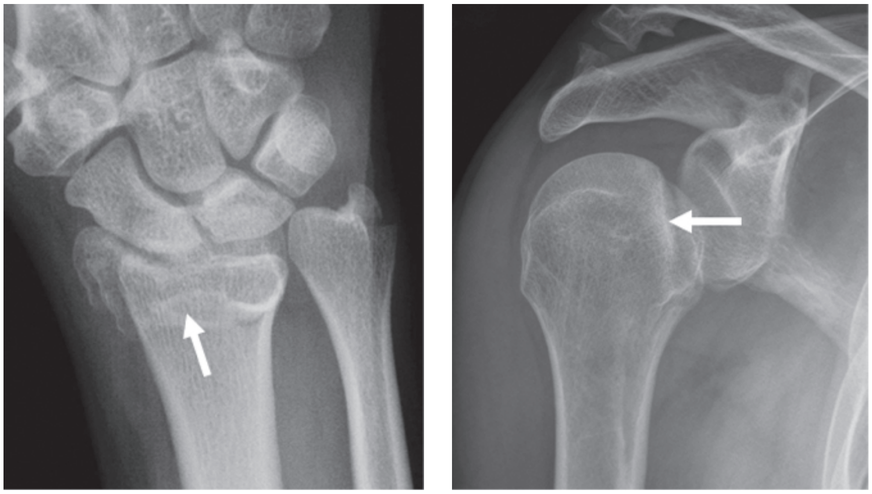

Figure 1.19 Sclerotic fracture lines related to impaction. (a) Distal radius impacted fracture shows a sclerotic line related to impacted trabeculae (arrow). (b) AP view of the shoulder shows a vertical sclerotic line (arrow) related to anteromedial humeral head impaction fracture in a patient with posterior dislocation.

Figure 1.20 Cortical buckling. Radial neck fracture shows focal cortical buckling (arrow). This finding may only be seen on one view and represents a fracture.

Angulation

Abnormal angulation may be the only manifestation of some fractures. For example, distal radial fractures may appear as loss of the normal minimal volar inclination of the distal radial articular surface (Figure 1.21) and distal humeral fractures may appear as loss of normal anterior angulation of the distal humeral metaphysis with respect to the shaft.

Trabecular malalignment

Proximal femur fractures can be subtle and appear as misalignment of trabeculae across the femoral neck (Figure 1.22). It is important to have an organized pattern approach to assess the cortical lines about the pelvis. Cortical disruption or an abrupt step-off along the ilioischial or ilipectineal line is a sign of a fracture of the pubic rami or the acetabular columns. Disruption of the sacral arcuate lines is a sign of a sacral fracture. These pelvic lines are described in greater detail in Chapter 7.

4. Assess the soft tissues

Soft tissues should be assessed on all musculoskeletal radiographs for swelling, gas, joint effusion and radiodense foreign bodies. Soft tissue swelling at some sites helps identify an underlying fracture. This is especially helpful when assessing trauma to the phalanges.

Tendons

One of the areas frequently overlooked on radiographs is the very anterior and very posterior soft tissues on lateral radiographs. Specifically, the quadriceps and the patellar tendon on the lateral knee radiograph, and the Achilles tendon on the lateral ankle radiograph. Injury to these superficial tendons is often visible radiographically, but only if one specifically and carefully evaluates these structures [28].

Fat pads

Displacement, obliteration or blurring of certain fat planes is also a helpful sign of an adjacent osseous injury. For example, the supinator fat pad may be obscured with radial head and neck fractures, the pronator fat pad with distal radial fractures, and the scaphoid fat pad with scaphoid fractures.

Joint effusions

The presence of a joint effusion in the acute setting in a patient with no underlying arthritis is a presumptive sign of a hemarthrosis. This blood may be the result of an intra-articular injury to either the soft tissues or adjacent bone. Radiographs are accurate in the detection of a joint effusion at the knee and the elbow. However, the accuracy of radiographs to detect joint effusion at other joints is

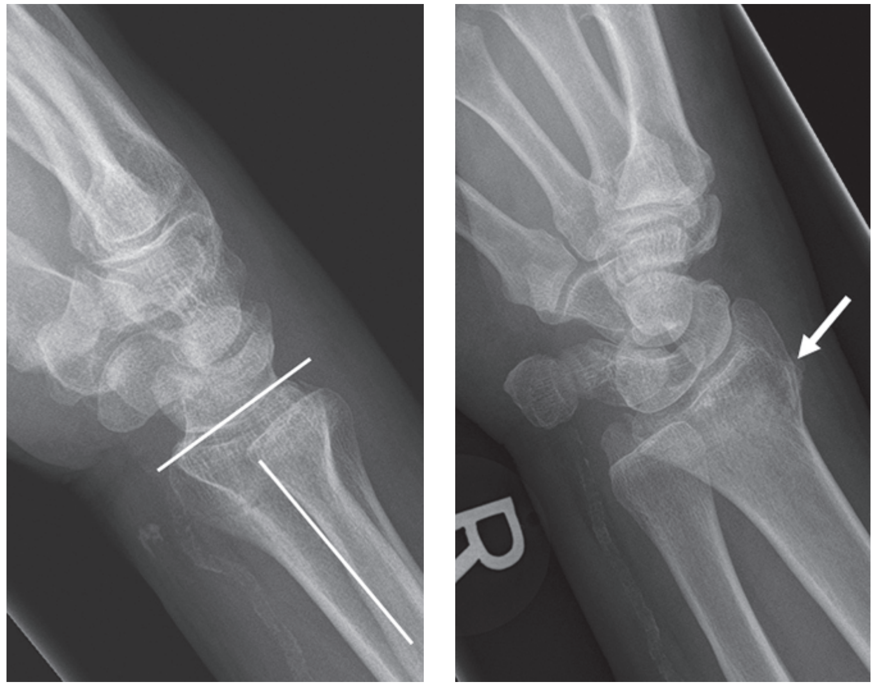

(a) (b)

Figure 1.21 Loss of normal angulation. (a) Lateral view shows loss of the normal volar angulation of the distal radial articular surface (line along the distal radial shaft and line along the distal radial articular surface show neutral alignment of the distal radial articular surface) compatible with a distal radial fracture. (b) Oblique view shows subtle sclerosis in the metaphysis related to impaction (arrow) at the fracture site.

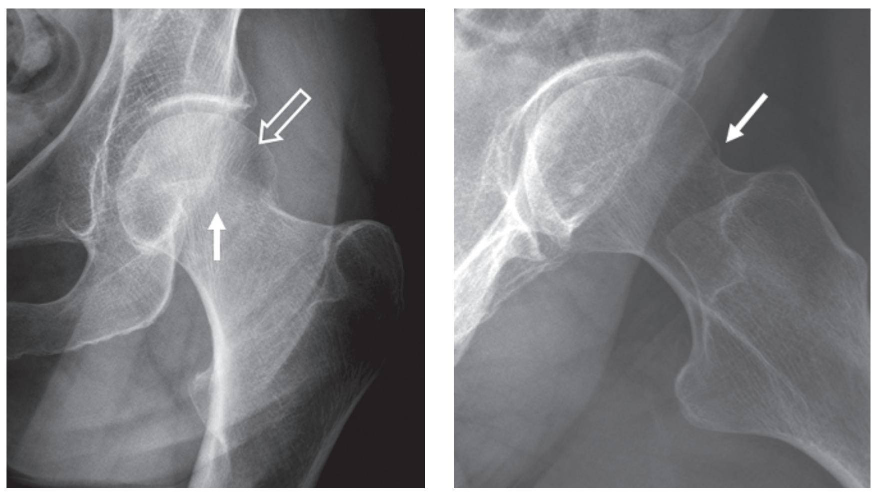

(a) (b)

Figure 1.22 Malalignment of the trabeculae across a subcapital fracture. (a) AP view shows valgus impaction across subcapital fracture evident by abrupt change in angulation of compressive trabeculae along the femoral neck (closed arrow) and femoral head (open arrow). (b) Frog-leg lateral view shows cortical disruption along the femoral neck (arrow).

limited. A cross-table lateral radiograph should be obtained in all patients with knee trauma to evaluate for the presence of fat within the joint, termed a lipohemarthrosis. This fat is displaced from the marrow into the joint in cases of an intra-articular fracture (Figure 1.23). The cross table radiograph will show a fat-fluid level in patients with a lipohemarthrosis.

Open fractures

Complex fractures, as well as fractures related to high-velocity energy, are more likely to be associated with an open wound. These fractures can also be referred to as compound or open fractures. It is important to assess for the presence of soft tissue gas on trauma radiographs (Figure 1.1(b)). The finding of gas directly impacts patient management, as these compound fractures require urgent open fixation. Other findings of an open fracture include a soft tissue defect, fracture fragment protruding beyond the expected soft tissues and radiodense foreign body material under the skin (Figure 1.24) [29]. The most common open fractures occur in the tibia (46%), followed by the femur (13%) and forearm (11%) [30]. It is therefore important to carefully inspect radiographs in patients with tibial fractures for evidence of an open fracture.

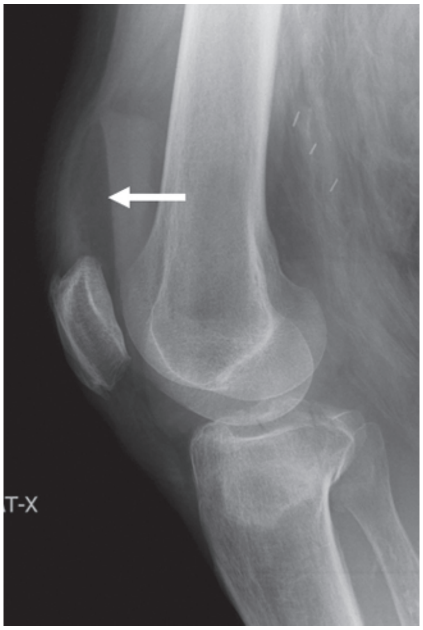

Figure 1.23 Lipohemarthrosis. Cross-table lateral radiograph shows a fat-fluid level (arrow) in the suprapatellar pouch. Sclerosis in the proximal tibia is related to a depressed tibial plateau fracture.

Foreign bodies

It is important to assess trauma radiographs for the presence of a radiodense foreign body (Figure 1.25). Foreign bodies may require surgical removal. The radiology technologist may place a marker at the skin to demarcate the site of the puncture. This facilitates detection of smaller radiodense foreign bodies.

5. Look for additional fractures and dislocations

It is important to remember that there may be several mechanisms of injury associated with a given traumatic event and this may result in more than one fracture. For example, a fall on an outstretched hand in the elderly may lead to concomitant humeral and radius fractures. It is important to assess adjacent joints for associated fractures. In the pelvis, and the foot, fractures are often multiple and the radiologist should not be satisfied after detecting one, or even several fractures. It is important to have an organized approach to assess all areas for a fracture. Checklists for each anatomic site are included in the chapters that follow.

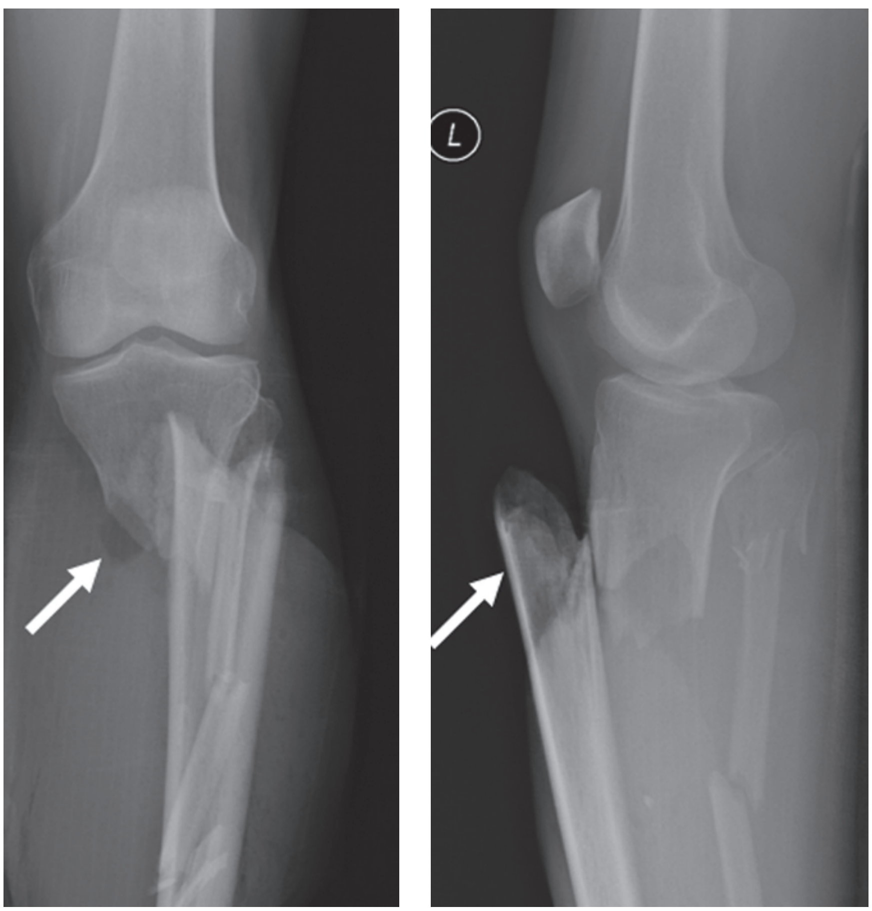

(a) (b)

Figure 1.24 Open fracture. (a) AP view shows soft tissue gas (arrow) and laterally displaced tibial and fibular fractures with overlap of fragments. (b) Lateral radiograph shows anteriorly displaced tibial fracture that protrudes through the skin (arrow).

Figure 1.25 Foreign body. A linear radiodense foreign body is shown adjacent to the fifth MTP joint (arrow). The technologist placed a paper clip adjacent to the foreign body entry site.

6. Assess for intra-articular fracture extension and joint alignment

Fractures that occur near a joint should be carefully assessed for the presence of articular fracture extension, articular step-off or gap (Figure 1.17). Joint alignment should be assessed on all views. Some joints, including the shoulder and the patellofemoral joint, often require special axial views to adequately assess alignment. Commonly missed joint dislocations on frontal radiographs include posterior shoulder dislocations, posterior hip dislocations, carpometacarpal dislocations, and tarsometatarsal (Lisfranc) dislocations. It is important to specifically assess for these dislocations and accompanying fractures.

Description of fractures and joint injuries

A complete description of a fracture should specify the precise anatomic location of the fracture, appearance of the fracture line, whether the fracture is open or closed, and fracture alignment and angulation. If the fracture involves a joint, congruence of the articular surface and alignment at that joint should be described. Accurate description of a fracture necessitates knowledge of appropriate terminology used to describe fractures and joint injuries. This terminology represents specific medical vocabulary that should be used correctly in order to facilitate effective communication between the radiologist and the clinician. The goal is to describe a fracture with enough accuracy that someone else could draw the fracture, without seeing the image itself.

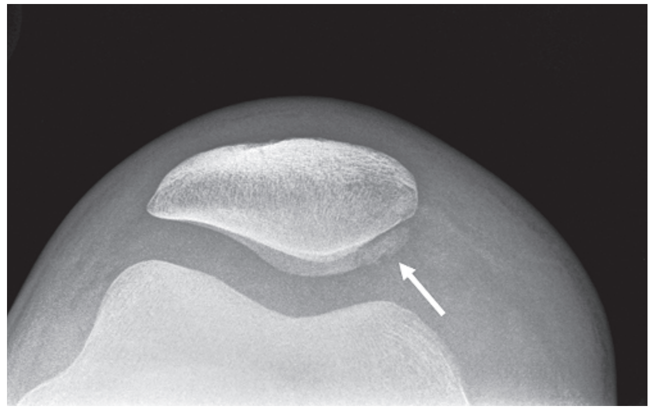

Figure 1.26 Osteochondral fracture. Axial view of the patella shows an osteochondral fracture along the medial patellar facet (arrow) in a patient with a prior transient lateral patellar dislocation.

Open versus closed

Use of the term closed or simple fracture is reserved for injuries with intact skin, while an open or compound fracture implies that the skin is disrupted (Figure 1.24). By definition, fractures caused by a laceration or a gunshot wound, as well as amputations are open fractures.

Location

Fracture location is described in terms of position in the bone. For long bones, the location is divided into proximal, mid and distal shaft. It should be specified whether the fracture extends to the joint surface, in which case it is intra-articular in location. Whenever possible, fracture location should be specified by including an anatomic point of reference such as the surgical neck of the humerus, the tibial plateau, or the metacarpal neck. For flat or irregular bones, examples of specific anatomic descriptors include the scaphoid waist or the scapular spine. These are discussed in chapters dedicated to specific anatomic sites.

Intra-articular extension

Intra-articular fractures may involve the articular cartilage only (chondral fracture), involve the bone and traverse the articular cartilage (transchondral fracture) or result in a fracture fragment that contains both the bone and articular cartilage (osteochondral fracture). Chondral and osteochondral fractures usually result from shearing or rotational impaction forces at a joint [31]. The fracture line is typically parallel to the joint, and it may be visible radiographically only if it contains a reasonable sized fragment of bone. This osteochondral fragment is often subtle radiographically (Figure 1.26). A pure chondral

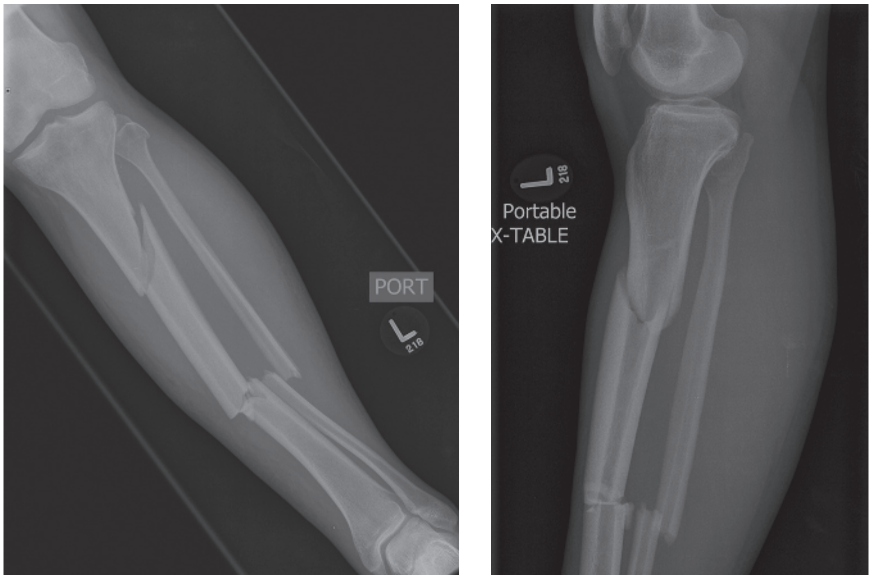

(a) (b)

Figure 1.27 Segmental fracture with angulation, displacement and overriding of fracture fragments. (a) AP and (b) lateral tibia–fibula radiographs show a segmental tibial fracture with valgus angulation at the distal fracture site. Companion distal fibular shaft fracture shows one shaft width anteromedial displacement and mild overriding of fracture fragments.

fracture may only be visualized on MR. Osteochondral injuries may accompany joint dislocations. Some examples of chondral and osteochondral injury following a joint dislocation include shoulder dislocation with resultant glenoid fracture, elbow dislocation with posterior capitellar fracture, hip dislocation with femoral head fracture, and patellar dislocation with medial patellar facet fracture.

Morphology of fracture lines

Fracture lines are often described in terms of their orientation as transverse (Figure 1.1), oblique (Figure 1.4), or spiral (Figure 1.5). Spiral fracture lines are by far the least common. In children (see Chapter 2), there are several unique fractures including bowing, torus, and greenstick fractures. A comminuted fracture contains more than two fracture fragments. Severity of comminution may be graded as minimal (small fracture fragments adjacent to dominant fracture line), moderate or severe (several large fracture fragments). If there is a dominant fracture fragment, it should be described in terms of size and displacement. A butterfly fracture is a subtype of a comminuted fracture with a wedge-shaped fracture fragment along the shaft of the bone (Figure 1.6). The location and any displacement of the fracture fragments should be described.

It is important to recognize a segmental fracture. This fracture type consists of two anatomically separate fracture lines along the shaft of the bone that isolate a middle segment of the bone (Figure 1.27). These fractures may be missed both clinically and radiographically, since the two fracture sites may be at a distance from one another. When describing segmental fractures, it may be helpful to describe fracture appearance at the proximal and distal fracture site separately, especially in cases of displacement and angulation. Some segmental fractures may be located on the opposite sides of a joint, and result in a "floating joint." Examples include a "floating elbow" with distal humeral and proximal ulna and radius fractures and a "floating knee" with distal femoral and proximal tibia and fibula fractures. Recognition of floating joint type segmental fracture facilitates appropriate treatment of these unstable injuries [32].

Alignment

The position of fracture fragments is described in terms of alignment and angulation. If these are all normal, the fracture is said to be nondisplaced, or in near anatomic alignment. Alignment is described in terms of position of the longitudinal axis of the distal fracture fragment with respect to the proximal fracture fragment. Loss of normal anatomic position is described as displacement. Additional descriptors include fracture apposition and rotation. Displacement should be graded in terms of shaft width (one quarter, one half, one shaft, or greater than one shaft width) (Figure 1.27(b)). The direction of displacement is described using two orthogonal views. The AP view is used to describe medial to lateral displacement and the lateral view to describe anterior to posterior displacement. Additional terminology is used at the wrist (volar, dorsal) and at the foot (plantar, dorsal).

Apposition

Apposition at the fracture site describes the extent of cortical contact between the fracture fragments. In cases of complete apposition, the fracture is nondisplaced. Fractures with two fracture fragments situated alongside

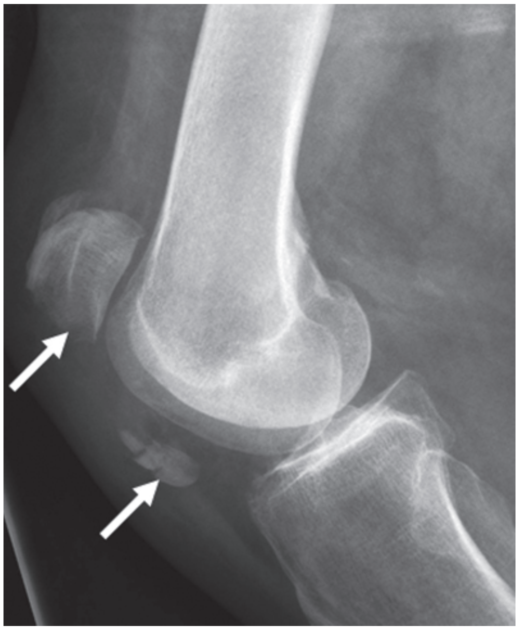

Figure 1.28 Distracted patellar fracture. Lateral radiograph shows significant separation of inferior pole and the remainder of the patella (arrows). The quadriceps tendon retracts the superior fracture fragment, and the patellar tendon retracts the inferior fracture fragment, with resultant patella alta.

of one another are described as overriding (Figure 1.27). Some fractures may be separated by a gap with no overlap, and are described as distracted. Distraction is common with transverse fractures that result from a tension force (patella, olecranon) or avulsion fracture related to a tendon pull (Figure 1.28). If there is overlap of the fracture fragments or distraction at the fracture site, these should be measured in millimeters or centimeters. Fractures can be impacted as well. Distracted or impacted fractures occurring in the lower extremity may lead to a leg length discrepancy if uncorrected.

Rotation

Rotation at the fracture site can only be assessed if both the joint proximal and distal to the fracture site are imaged on the same radiograph (Figure 1.29). In cases where one joint is seen in AP projection and the other joint in lateral projection, rotation is described as 90 degrees. Another clue to rotation is significant disparity between the diameter of the proximal and distal fracture shaft, suggesting that they are profiled at a different angle on the radiograph [33].

Angulation

It is important to appreciate that description of fracture alignment is separate from description of angulation. A fracture may be severely displaced, with no angulation, or conversely, it may be severely angulated with no displacement or loss of contact at the fracture site. By convention, angulation is described in terms of position of the distal fragment with respect to the proximal fragment (rather than the position of the apex of angulation). It is important to use two orthogonal views to describe fracture angulation (Figure 1.27). The AP view provides information regarding angulation in the coronal plane including medial and lateral at most fracture sites and radial and ulnar at the forearm. The terms varus and valgus are often used in lieu of medial and lateral. Varus refers to angulation of the distal fragment towards the midline of the body and valgus away from the midline (Figure 1.30). The lateral view provides information regarding angulation in the sagittal plane including anterior and posterior at the humerus, femur, tibia and fibula, volar and dorsal at the wrist, and plantar and dorsal at the feet. Measurements in terms of degrees of angulation are helpful for the clinician to guide management. The fracture may be angulated in two planes, for example anteromedial or posterolateral. Angulation in the plane of motion of a joint is less debilitating than angulation outside the plane of motion of joint. Therefore varus or valgus is usually the worst type of angulation for future limb function.

Impaction

Some fractures may be impacted and it is important to grade the severity of impaction by providing a measurement. It may be difficult to directly measure impaction of a distal radial fracture. In those cases, indirect measurement with respect to ulnar shaft length is used to infer the severity of impaction. This measurement is provided in terms of ulna variance; positive ulna variance indicates impaction at the radial fracture site. Ulnar variance is further discussed in Chapter 6.

Avulsion

Avulsion fractures are caused by abnormal tensile stress on ligaments or tendons [34]. These fractures occur at typical locations in the hands (dorsal distal phalanx with extensor tendon avulsion), feet (base of fifth metatarsal with peroneus brevis avulsion), and pelvis (ischial tuberosity with hamstring tendon avulsion). The avulsed fracture fragment may be purely cartilaginous, osteocartilagenous, or most commonly, just osseous. The latter two avulsion fractures are visible radiographically. The size of the fragment varies, and the degree of displacement also varies. Some avulsion fractures may be subtle, with displacement of a tiny ossific fragment. It is important to look for associated soft tissue swelling, especially at the digits, and joint alignment to infer ligament or tendon injury (ACL avulsion and anterior translocation of the tibia with respect to the femur). MR is more sensitive than radiographs to identify and characterize these injuries. Some avulsion fractures should be presumed pathologic

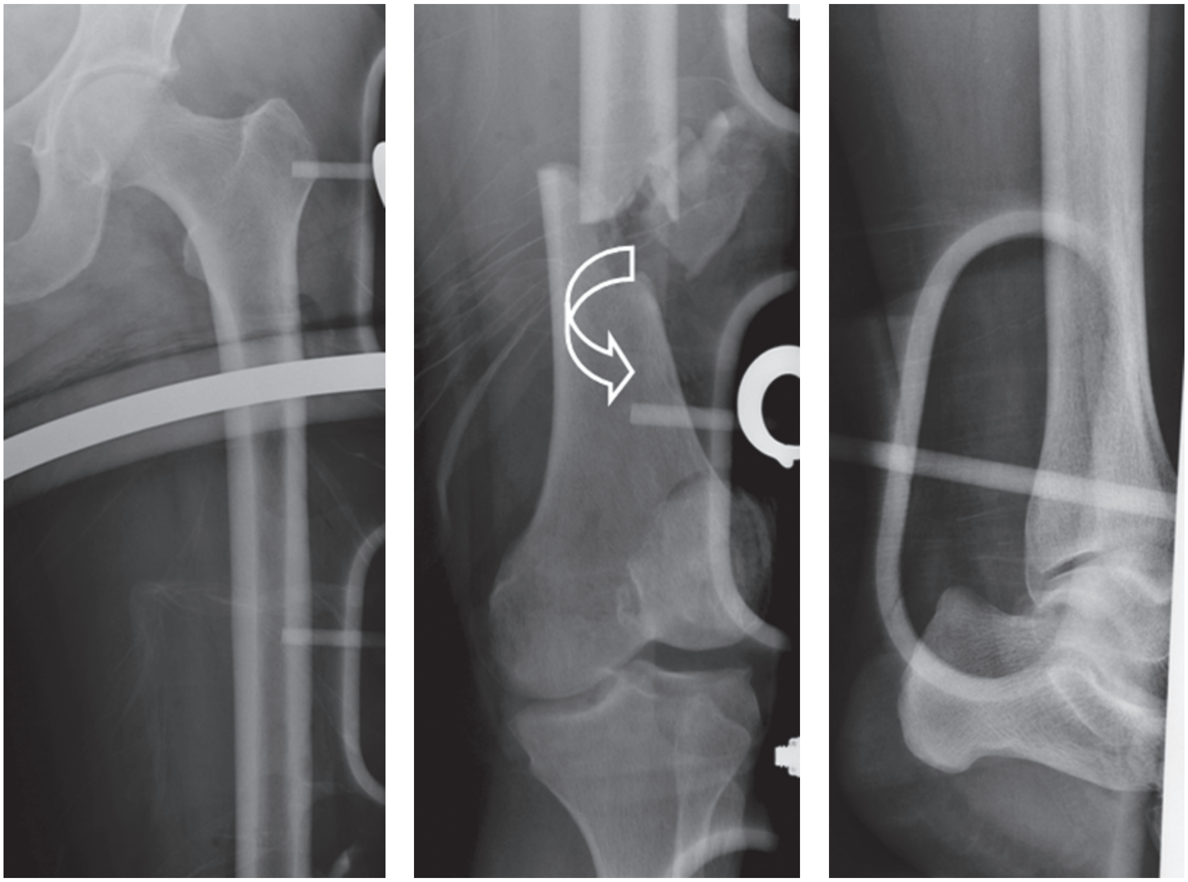

Figure 1.29 External rotation across a fracture. (a) AP view of the proximal and (b) distal femur shows an oblique distal femoral shaft fracture with one half shaft width medal displacement and external rotation (curved arrow). (c) AP view of the ankle shows the ankle in lateral projection related to external rotation at the distal femoral fracture site. Traction device is in place across the fracture.

until proven otherwise. These include lesser trochanter avulsion or avulsion at an atypical site such as the distal humeral epicondyle (Figure 1.31) in adults.

Joint alignment

Abnormal alignment at a synovial joint is described either as subluxation if there is partial contact between the articular surfaces, or dislocation, if there is no contact between the opposing articular surfaces (Figure 1.32). The severity of subluxation may be described in terms of percentage of articular congruity. A common error in description terminology is to describe a joint as displaced, a term which should be used only for a fracture. The convention of naming the dislocation depends on the size of the bones involved at a joint. For example, if the major bones at a joint are involved, such as with tibiofemoral dislocation, the injury is called a knee dislocation. If a smaller bone is involved at a joint with several bones, the injury is called according to the bone that is in an abnormal position (ex. patellar dislocation, lunate dislocation). It is important to recognize soft tissue gas about a dislocation. An open dislocation is a surgical emergency that requires urgent closure to prevent septic arthritis and potential devastating joint destruction [35].

Abnormal alignment at a synarthrodial or partially mobile joint is termed diastasis. Commonly involved joints include the symphysis pubis and the sacroiliac joint. There are often associated fractures either adjacent to the joint or extending into the joint (Figure 1.33).

Spine alignment

Alignment on spine radiographs should be described in both the coronal and sagittal plane. Kyphosis and acute lordosis should be described on the lateral radiograph, and dextro- or levoscoliosis on frontal radiographs. Rotatory abnormality may be present on both the lateral and frontal radiographs. Listhesis is defined as abnormal slippage of one vertebral body with respect to the other, and is usually described in terms of the body above with respect to the body below.

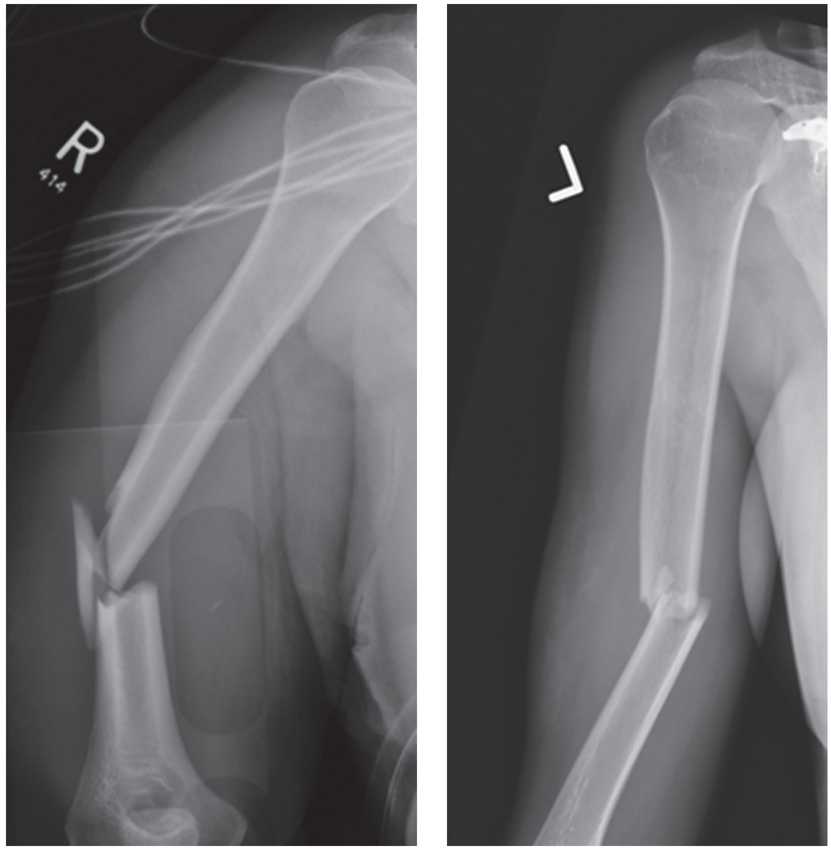

(a) (b)

Figure 1.30 Varus and valgus angulation. (a) Varus angulation across bending wedge distal humeral fracture. (b) Valgus angulation across oblique mid-humeral shaft fracture.

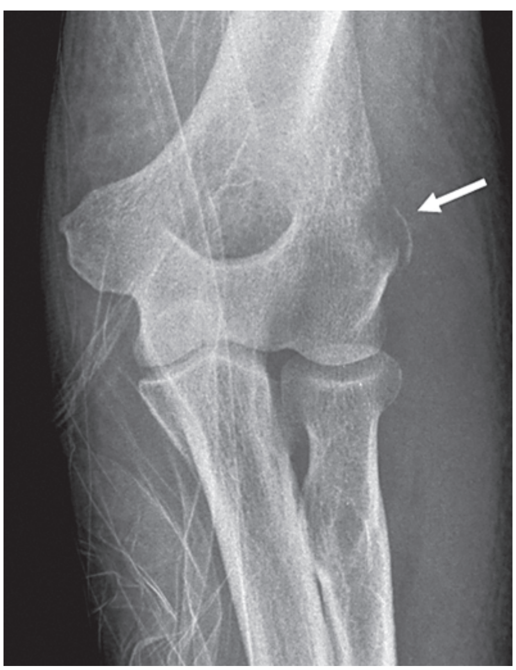

Figure 1.31 Pathologic avulsion fracture. AP radiograph of the elbow shows an avulsion fracture at the lateral epicondyle of the distal humerus (arrow) with an underlying lytic lesion.

Retrolisthesis represents posterior displacement of the body above with respect to the body below. For example, "retrolisthesis of L2" refers to an abnormality occurring at L2-3. Anterolisthesis is usually described as "anterolisthesis at L2-3" if the abnormality occurs at L2-3.

Anterolisthesis is graded in the lumbar spine on a scale 1-4 based on the percentage of body slippage (1 = 0–25%, 2 = 25–50%, 3 = 50–75%, 4 = greater than 75%). In the cervical spine, anterolisthesis is simply described in terms of absolute measurement, or a percentage of vertebral body displacement.

Lateral listhesis should be described by reviewing frontal radiographs in terms of the position of the body above with respect to the body below. For example "left lateral listhesis of L2 with respect to L3". Description of alignment in the spine is discussed in greater detail in Chapter 3.

Classification of fractures

Accurate fracture description is usually sufficient to guide patient management. Classification systems have been developed to stratify patients into different treatment categories, grade the severity of the injury and predict outcomes. There are specific classification systems for each fracture site and these are described in subsequent chapters.

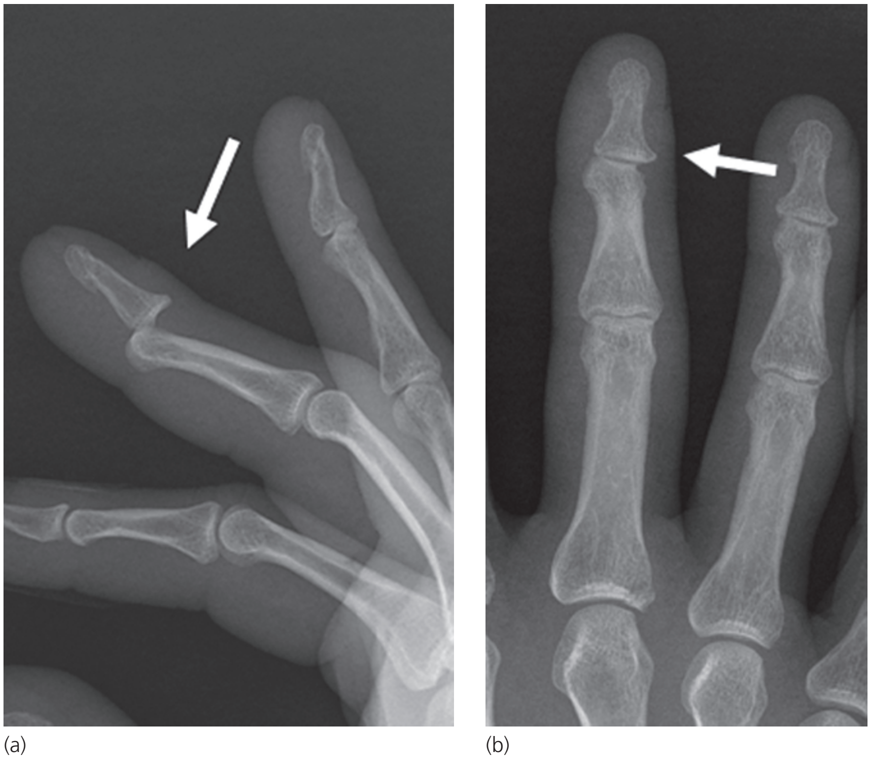

Figure 1.32 Dislocation at the distal interphalangeal joint. (a) Lateral and (b) PA radiographs show a dorsal dislocation and the DIP joint to the long finger (arrows).

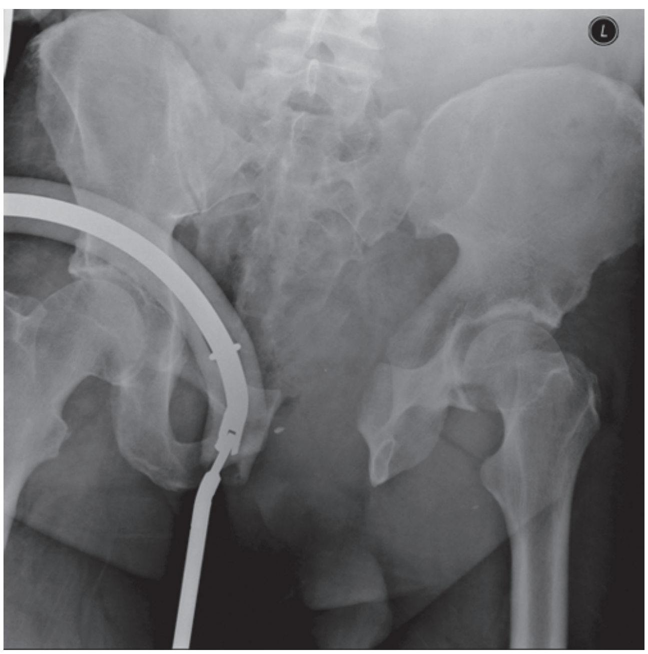

Figure 1.33 Diastasis of the left sacroiliac joint and the symphysis pubis.

The most common classification system used by orthopedic surgeons is the Mueller AO Classification system [36]. This classification system was developed to provide consistency in long bone fracture classification, with the goal to standardize research across institutions. This classification system is detailed, and it can be applied to most fracture sites (Figure 1.34). It is arranged in order of increasing severity according to fracture complexity, difficulty of treatment and worsening prognosis. Note that the classification system differs for end-of-bone versus middle segment fractures. Middle diaphysis segment fractures can be either simple (one fracture line with >90% cortical contact after reduction), wedge (three or more fragments, main fragments have contact after reduction) or complex (three or more fragments, main fragments have no contact after reduction). End-of-bone fractures can be either extra-articular, partial articular (part of the articular component involved, while the other part is attached to metadiaphysis) or complete articular (metaphyseal fracture component completely separates the articular component from the diaphysis).

Special types of fractures (stress, insufficiency, and pathologic)

There are special types of fractures other than the typical injury to normal bone from acute trauma. These special fractures are termed stress, insufficiency, and pathologic fractures. Incorrect use of terminology with respect to these fractures is unfortunately common.

Stress fractures

Definition: *A stress fracture is a fracture through bone as a result of abnormal, repetitive and persistent stress. If the bone is normal, this is termed a fatigue fracture; if the bone is systemically abnormal, it is termed an insufficiency fracture.*

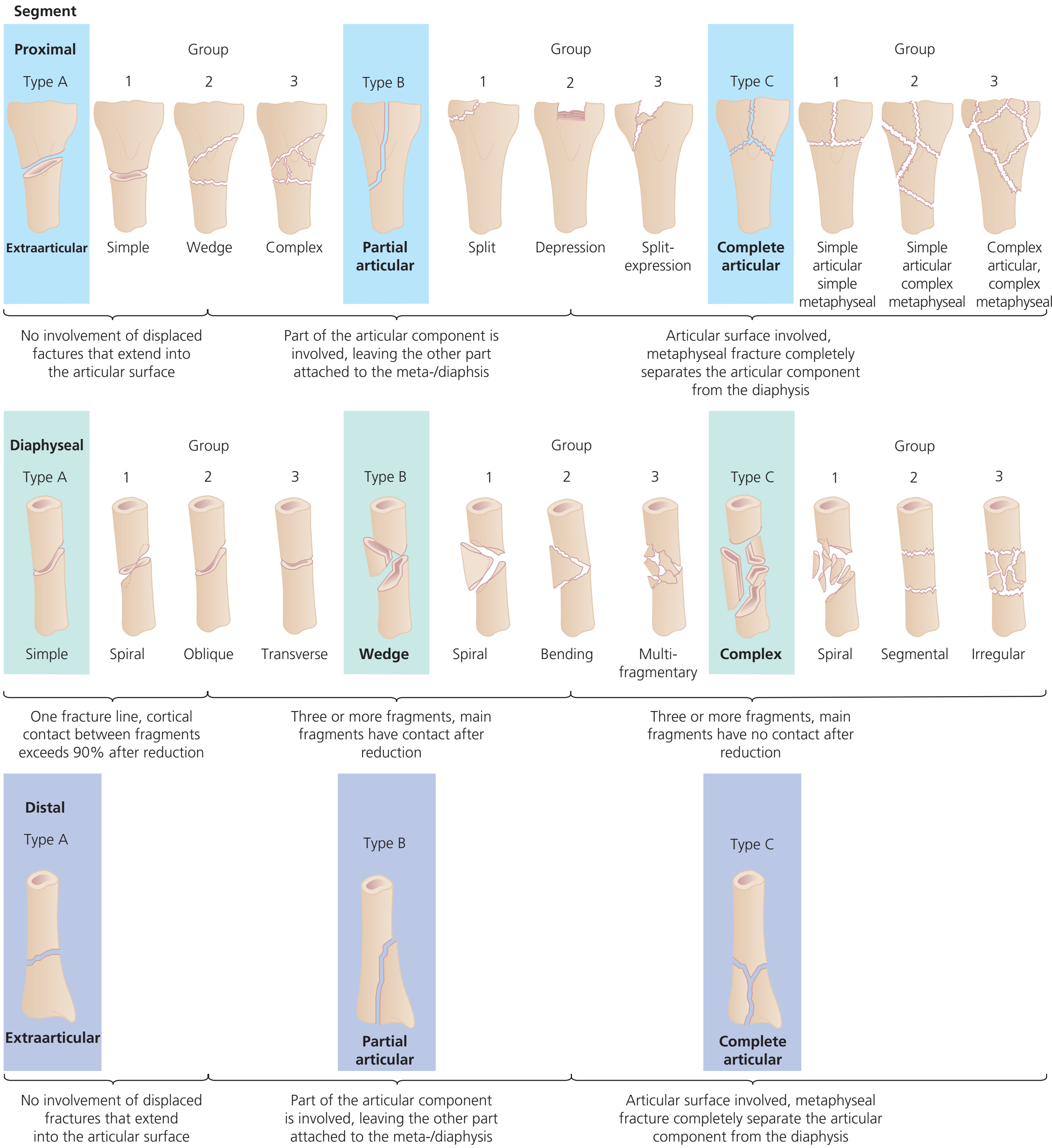

Figure 1.34 AO classification of long bone fractures. The classification system is based on fracture location (proximal, distal or diaphyseal), articular involvement and severity of fracture fragmentation. Modified from www.aofoundation.org with permission.

Epidemiology

The triad associated with most stress fractures includes: 1) activity is new or different for the individual, 2) strenuous, and 3) repeated with a frequency that ultimately produces symptoms [37]. Examples of activities include new exercise routine or occupational work (Table 1.1) [38, 39].

The amount of increased load on the bone may vary between patients. A sedentary individual may sustain a stress fracture after commencing a new training program of daily walking, or a competitive marathon runner may sustain a stress fracture by doubling the running distance during daily running regimen. Patients typically present with pain that occurs during activity and resolves after the activity stops.

Location

The likelihood of a stress fracture is dependent on the quality of the bone, the magnitude of stress, and the frequency and time period during which the stress is applied [39]. The location of stress fractures is quite typical with certain activities. For example, running is associated with stress fractures of the second and third distal metatarsal shaft, posterior calcaneus, distal tibia or fibula shaft, femoral neck and pubic ramus. Midfoot stress fractures are also common in runners and dancers, especially the navicular and cuneiforms [40, 41].

Table 1.1 Location and causes of common stress fractures

Location of stress fracture	Inciting activity
Metatarsal shaft	Running, marching, hallux valgus surgery, ballet dancing
Sesamoids	Prolonged standing
Calcaneus	Jumping, prolonged standing, recent immobilization
Tibia and fibula shaft	Running, especially long distance
Patella	Hurdling
Femur neck and shaft	Running, ballet dancing
Pelvis (pubic rami)	Gymnastics, running
Pars interarticularis	Gymnastics, ballet dancing
Ribs	Rowing, carrying a heavy pack, coughing
Hook of hamate	Golf, tennis, baseball

Modified from Daffner and Pavlov [42] with permission from American Roentgen Ray Society.

Complications

Some stress fractures are considered high risk injuries because of their propensity to result in delayed union or nonunion [42]. Examples include stress fractures involving the femoral neck (especially laterally), anterior tibial cortex, navicular, fifth metatarsal shaft and the sesamoids [43, 44]. These fractures should be recognized early to ensure prompt diagnosis and treatment. Delay in treatment may result in complete fracture of a long bone or opposite bone secondary to altered weight bearing. Low risk stress fractures usually heal without complications following cessation of activity. These include rib fractures, pubic rami fractures, femoral shaft, metatarsal shaft (other than fifth) and most pars interarticularis fractures [45].

Imaging evaluation

Radiographs in stress fractures may be initially negative in up to 80% or patients and remain negative in up to 60% of patients [46]. Despite the low sensitivity, radiographs are recommended as the initial imaging study. If the findings are present, no further imaging is necessary. The imaging appearances of stress fractures are varied. The fracture may appear as a faint lucent line, or somewhat more commonly as a band of linear sclerosis perpendicular to the trabeculae (Figure 1.35), endosteal sclerosis, or longer segment periosteal reaction (Figure 1.36).

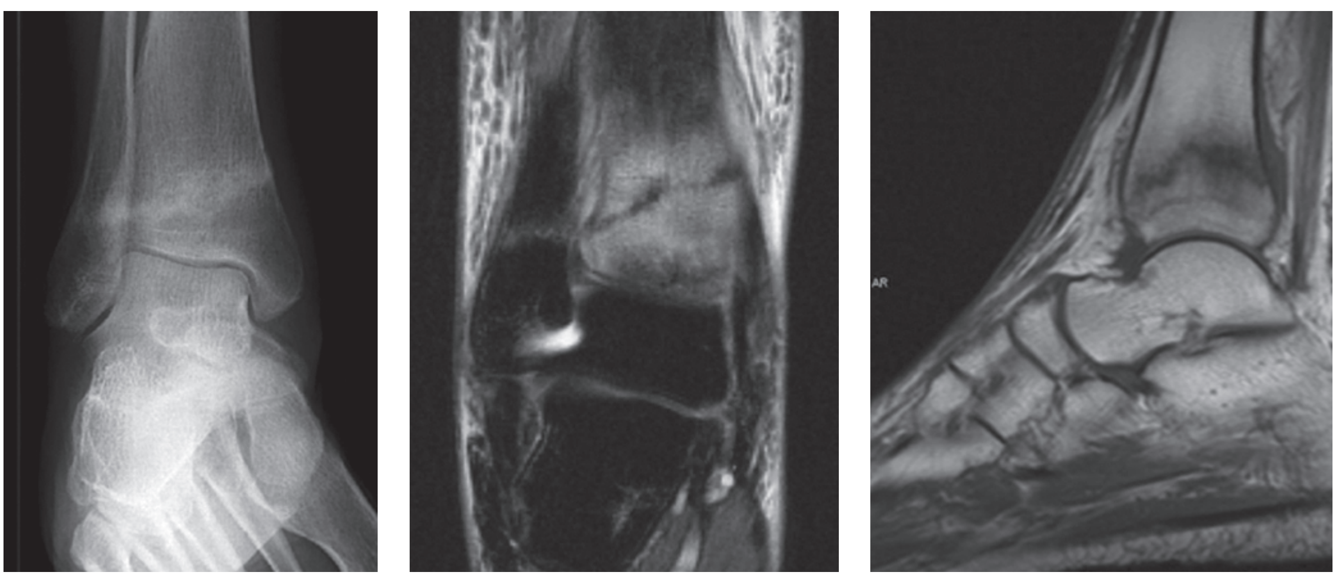
(a) (b) (c)

Figure 1.35 Tibial and fibular stress fractures. (a) Oblique ankle radiograph shows linear, oblique sclerotic lines in the distal tibia and fibula. (b) Coronal fat-suppressed proton density image shows the low signal fractures in the distal tibia and fibula with adjacent marrow edema, more marked in the tibia. (c) Sagittal T1-weighted image shows the low signal intensity tibial fracture line. T1-weighted images are best at depicting the fracture line.

Figure 1.36 Stress fracture of second metatarsal shaft. AP radiograph shows periosteal reaction at the medial margin of the distal second metatarsal shaft (arrow).

MR is the imaging method of choice to identify stress fractures in patients with negative radiographs. The T1-weighted images show a low signal intensity line with surrounding edema on T2-weighted images (Figure 1.35(b) and (c)) [47].

A bone scan may also be useful in patients where MR is contraindicated or not available. The advantage of a bone scan is the ability to detect additional, usually contralateral stress fractures that may be asymptomatic during the examination [48]. The sensitivity of bone scan and MR are similar. A negative bone scan in a patient with suspected stress fracture generally excludes a diagnosis of a stress fracture, and the patient may return to normal activity.

CT may be also used in patients with contraindications to MR [49]. In long bone stress fractures, images will show a lucent fracture line with or without periosteal reaction, depending on the age of the fracture. Axial plane alone may not show the fracture, and multiplanar reformatting is required. CT is of greater importance in detection of stress fractures of the pars interarticularis in the lower lumbar spine. These fractures usually occur in adolescent gymnasts.

Insufficiency fractures

Definition: *An insufficiency fracture results when a weakened bone is subjected to normal activities. These fractures are usually seen in patients whose bones are weakened as a result of osteoporosis or a disease process, or both (Box 1.1). The diffuse abnormality of the bone, and the repetitive nature of the injury distinguish insufficiency fractures from pathologic ones*.

Box 1.1 Risk factors for insufficiency fractures

- Osteoporosis
- Corticosteroid use
- Bisphosphonate therapy
- Rheumatoid arthritis
- Radiation treatment
- Osteomalacia or rickets
- Renal osteodystrophy and hyperparathyroidism
- Diabetes mellitus
- Osteogenesis imperfecta
- Osteopetrosis
- Scurvy
- Paget's disease
- Ankylosing spondylitis

Epidemiology

The most common populations to be affected by insufficiency fractures include elderly persons with osteoporosis, patients with rheumatoid arthritis, renal osteodystrophy, individuals using corticosteroids, or bisphosphonates [50], or those who underwent radiation therapy. The osteoporotic bone is characterized by thinning of both the cortex and trabeculae with resultant decrease in bone mass. Patients with rheumatoid arthritis are at increased risk for insufficiency fractures because of the osteopenia related to the inflammatory hyperemic aspects of the disease, corticosteroid therapy, deformity of extremities, as well as the joint replacements that facilitate new activity [51]. Renal osteodystrophy and hyperparathyroidism are characterized by loss of calcium and resultant decrease in normal mineralization of osteoid matrix, leading to decreased biomechanical bone quality. Radiation treatment weakens bone in a population that is usually elderly with underlying osteoporosis, further increasing the risk for an insufficiency fracture. Additional risk factors for insufficiency fractures include ankylosing spondylitis, osteomalacia and rickets, osteogenesis imperfecta, and Paget's disease. It is important to differentiate insufficiency fractures from pathologic fractures discussed below. Pathologic fractures occur through a bone that is focally replaced by abnormal soft tissue.

Location

The typical sites for insufficiency fractures in osteoporotic patients include the proximal humerus, distal radius, vertebral body, femoral neck, pubic body, pubic ramus, sacrum and ilium. Iliac fractures may occur through the supra-acetabular ilium in a horizontal plane, iliac blade,

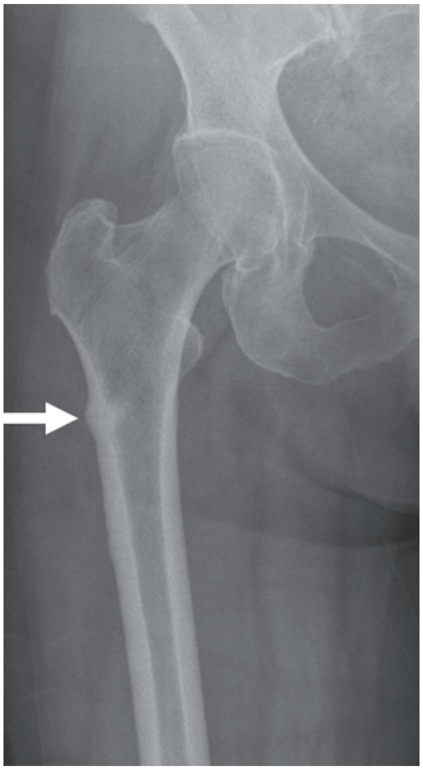

Figure 1.37 Insufficiency fracture in a patient on bisphosphonate therapy. AP radiograph shows focal lateral cortical thickening involving the lateral proximal femoral shaft (arrow).

or superomedial ilium parallel to the sacroiliac joint [52]. The presence of an insufficiency fracture should prompt consideration of anti-osteoporotic therapy.

Imaging evaluation

The current recommendations for imaging patients with suspected insufficiency fractures suggest initial evaluation with radiographs. In many instances the fracture will be apparent radiographically. MR is the imaging modality of choice if radiographs are negative and a fracture is suspected. CT is often helpful to confirm the diagnosis in cases of insufficiency fractures of the sacrum and pelvis. Bone scan is sensitive for detection of insufficiency fractures in majority of patients within 24 hours of symptom onset. It may be falsely negative in osteoporotic patients and in those using corticosteroids [42].

Radiographic findings in long bone fractures may be subtle and usually appear as a sclerotic line perpendicular to trabeculae (Figure 1.14(b)). Proximal femoral shaft fractures in patients on bisphosphonate therapy are important to recognize early [50]. These fractures may initially show focal cortical thickening with or without underlying fracture lucency (Figure 1.37). Bisphosphonate therapy-related fractures are at risk to progress to complete displaced fractures and may result in significant morbidity.

Insufficiency fractures in the pelvis typically appear as vertical subtle sclerosis in the sacral ala, fracture through the pubic ramus or patchy sclerosis and lucency in the pubic body (Figure 1.38(a)). Not infrequently, insufficiency fractures in the pelvis may be confused for metastatic lesions, especially if resorption occurs at the fracture ends [52]. The most common location for insufficiency fractures to be confused with metastatic foci is the acetabulum. These fractures often occur in elderly patients with a history of malignancy, possibly also including treatment with radiation, which further increases the risk of insufficiency fracture. MR may be the first imaging study in that setting and the imaging appearance may be attributed to metastases (Figure 1.38(b)). The typical location and the presence of a low signal intensity fracture line should facilitate correct diagnosis of an insufficiency fracture. In equivocal cases, CT may help identify the fracture line and confirm the diagnosis of an insufficiency fracture (Figure 1.38(c) and (d)) [52].

Vertebral body insufficiency fractures are compression fractures that may result in kyphosis of the thoracic spine. The fracture is typically axially oriented and the compression at the fracture site results in linear sclerosis and collapse. The imaging appearance of an osteoporosis-related compression fracture may be mistaken for a pathologic fracture from malignancy. There are several imaging features that may help distinguish insufficiency from pathologic vertebral body compression fractures on imaging, including MR (Table 1.2) (Figures 1.39 and 1.40) [53]. These include location of the fracture, orientation and presence of the fracture line, the absence of a large soft tissue mass, absence of bulging of the posterior cortex, lack of involvement of posterior elements, consecutive involvement and greater superior as opposed to inferior endplate depression. The use of in-phase and out-of-phase sequences is helpful in differentiating benign insufficiency fractures from pathologic fractures in the spine [54]. Inversion recovery sequences can be helpful in that they are more likely to demonstrate not only the edema pattern, but also the fracture lines themselves [55]. CT can further help identify and characterize the fracture line. The presence of gas in the fracture on CT confirms the diagnosis of an insufficiency fracture (Figure 1.39(c)).

Pathologic fractures

Definition: *A pathologic fracture occurs through a bone that is focally replaced by abnormal tissue and injured following a low-energy vector*.

Epidemiology

Common pathologic processes that may result in a pathologic fracture include metastatic bone disease, lymphoma, multiple myeloma, benign bone tumors (unicameral bone cyst, enchondroma), and rarely infection (Figure 1.41).

Location

There are predictable locations for pathologic fractures, with most occurring in the spine, femur and humerus [56, 57].

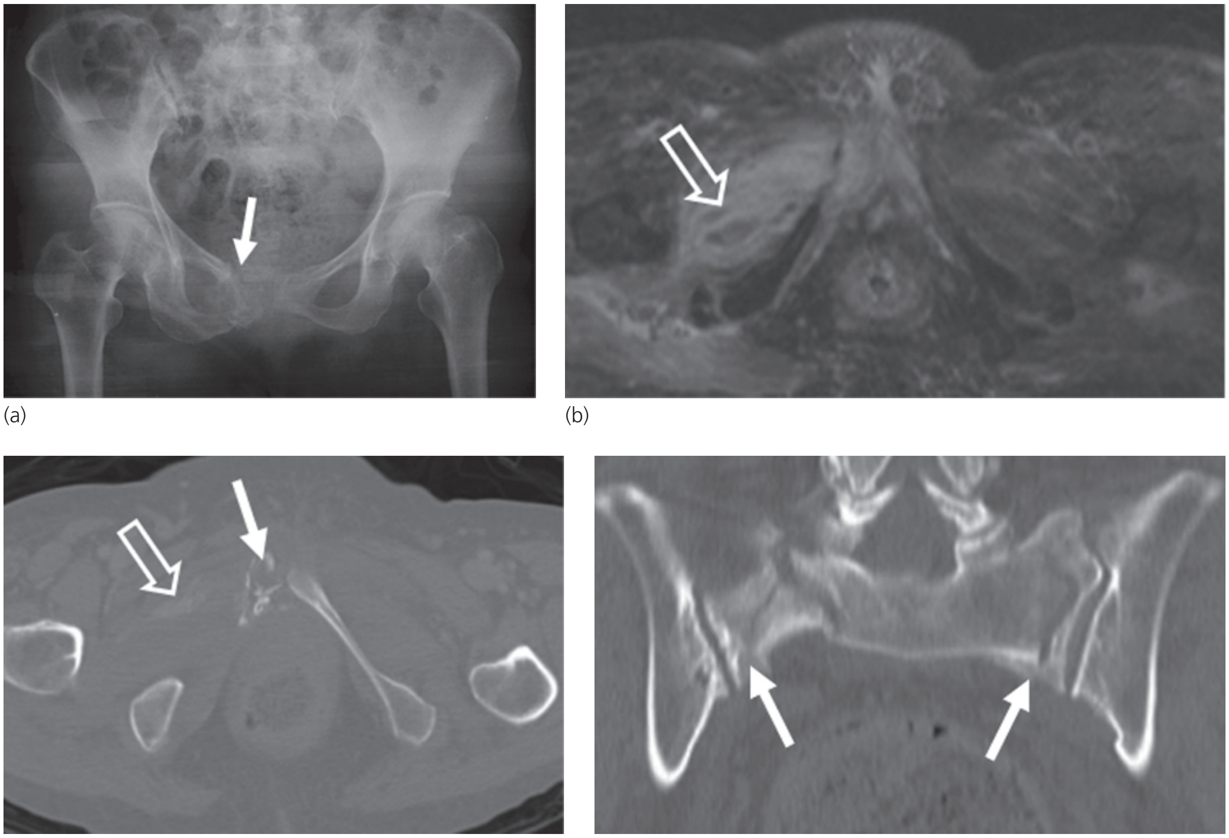
(a) (b) (c) (d)

Figure 1.38 Pelvic insufficiency fractures. (a) AP radiograph shows a right pubic body and adjacent pubic rami healing fractures (arrow) evident by patchy sclerosis and lucency. (b) Axial T2-weighted, fat-suppressed image shows soft tissue edema and central low signal areas (open arrow) in the region of right adductor musculature. (c) Axial CT image shows the right pubic body fracture (closed arrow) and heterotopic ossification (open arrow) in the adductor musculature corresponding to the low signal region on MR in (b). (d) Coronal reformatted CT image shows associated sacral ala fractures bilaterally (arrows).

Table 1.2 Distinguishing MR features between insufficiency and pathologic fractures in the spine

Feature	Insufficiency fracture	Pathologic fracture
Location	T7 and below	Dens
	Most at T10–L4	Upper thoracic spine
	Most common at L2	L5 common
Sequential	Yes	No
Posterior elements	No	Yes
Fracture line	Horizontal	Vertical
Posterior bulging	No	Yes
PLL avulsion	Yes	No
Endplate involvement	Superior > inferior	Inferior > superior
Soft tissue mass	No	Large

PLL = posterior longitudinal ligament.

Fractures through the femoral shaft and subtrochanteric region should be carefully inspected for the presence of an underlying osseous lesion. Certain fractures should be considered pathologic until proven otherwise including avulsion fracture of the lesser trochanter in adults (Figure 1.42) or humeral diaphysis fracture in the absence of significant trauma.

In the spine, pathologic fractures result in compression of the vertebral body [53]. The fractures are often multiple, involve nonconsecutive levels, and the pathologic process involves the pedicles. Imaging features that help distinguish pathologic fractures from osteoporotic vertebral fracture are listed in Table 1.2.

Imaging evaluation

Radiographs of a pathologic fracture in the long bone show a fracture through a discrete focal osseous lesion, and the diagnosis is obvious. The cortex is usually thinned, expanded or destroyed (Figure 1.41(a)). In some cases, the displaced fracture obscures an underlying lytic lesion. It is important to consider clinical history of minor

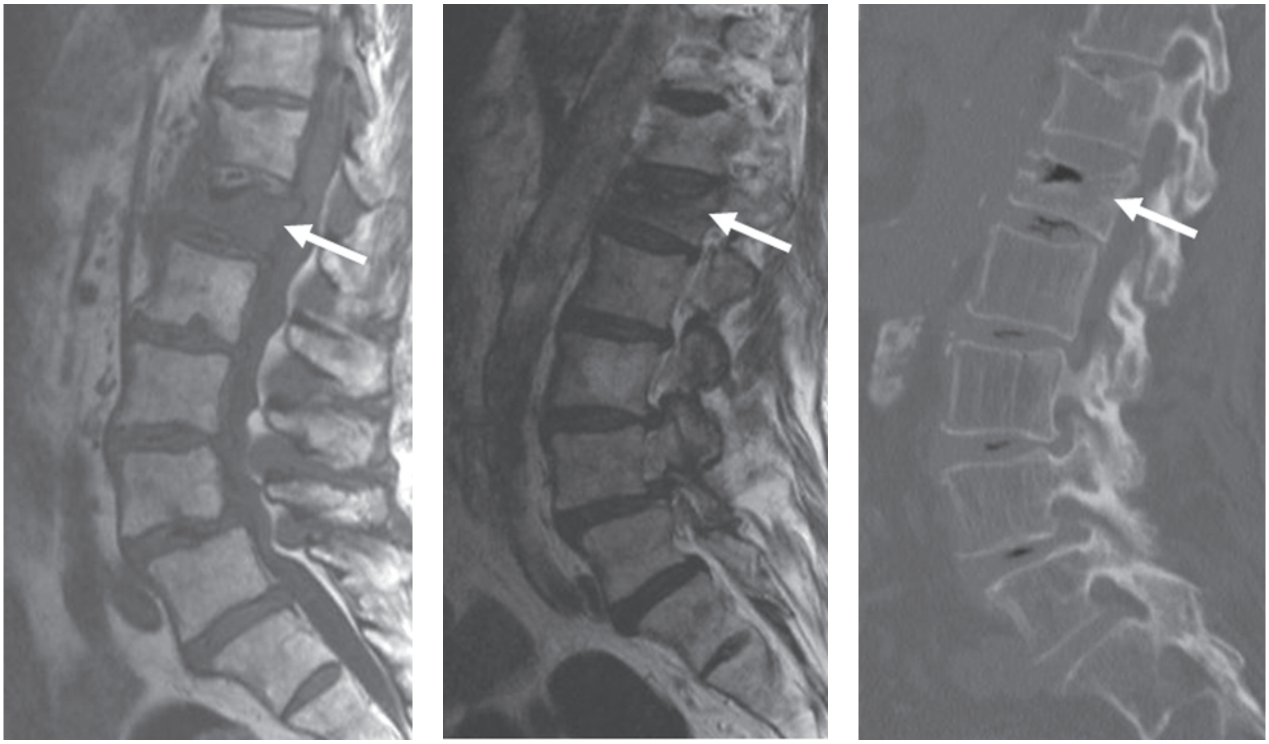

(a) (b) (c)

Figure 1.39 Insufficiency vertebral body fracture. (a) T1- and (b) T2-weighted images show L1 low marrow signal with superior endplate compression and horizontal fracture line (arrow in b). (c) Sagittal CT reformatted image shows gas in the fracture cleft (arrow) compatible with an insufficiency fracture.

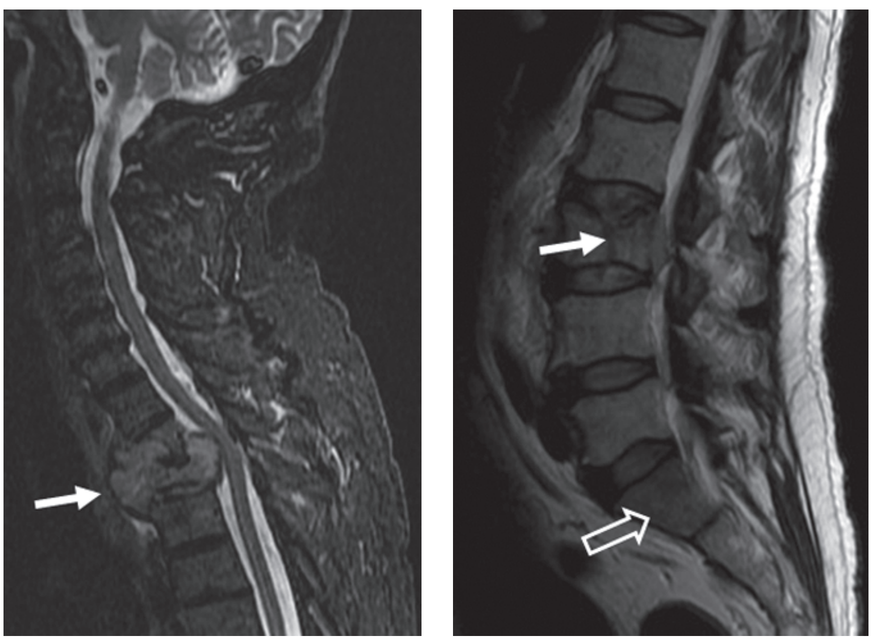

(a) (b)

Figure 1.40 Pathologic vertebral compression fractures. (a) Sagittal inversion recovery image shows a large mass replacing the upper thoracic vertebral body (arrow) with vertebral height loss and posterior epidural mass compressing the cord. (b) Sagittal T2-weighted image in a different patient shows an L3 vertical fracture (closed arrow) with a small epidural mass posterior to the body. An additional marrow-replacing lesion is seen in the sacrum (open arrow).

trauma to diagnose those fractures as pathologic. An additional imaging clue may be the inability to visually connect the two fracture fragments related to underlying osseous destruction. The orientation of fracture line in pathologic fractures is typically transverse. When a transverse long bone fracture is identified in the absence of significant trauma, a pathologic fracture should be considered as the primary diagnosis.

It is important not to mistake healing fractures for a pathologic fracture. Resorption at the fracture site and

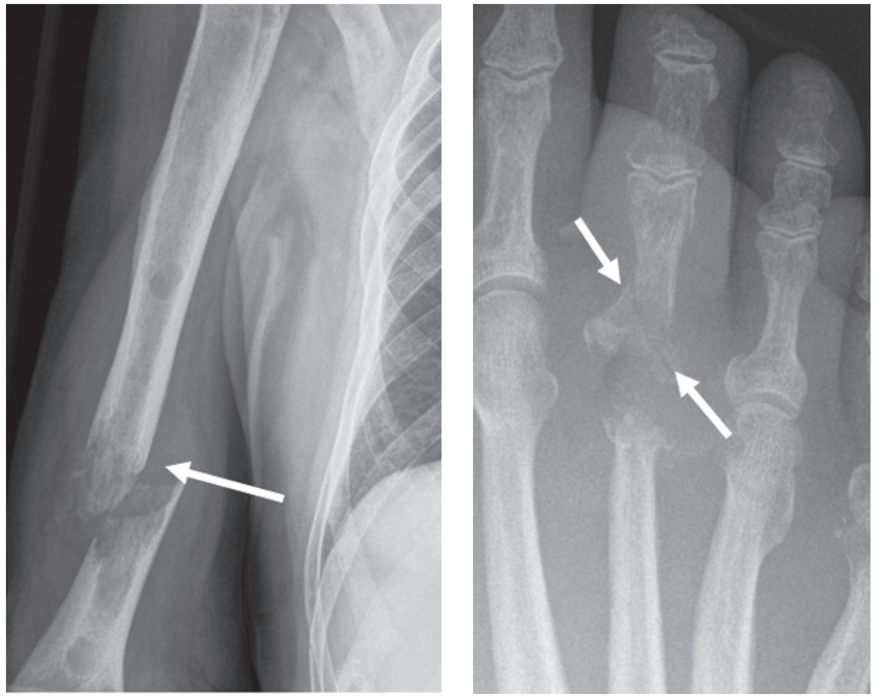

(a) (b)

Figure 1.41 Pathologic fractures. (a) Pathologic fracture through the distal humeral shaft through an underlying destructive, permeative lytic lesion (arrow). There are additional lytic lesions in the remainder of the humeral shaft in this patient with multiple myeloma. (b) Pathologic fracture through osteomyelitis and septic arthritis at the third MTP joint. The fracture is obliquely oriented through the proximal phalanx base (arrows).

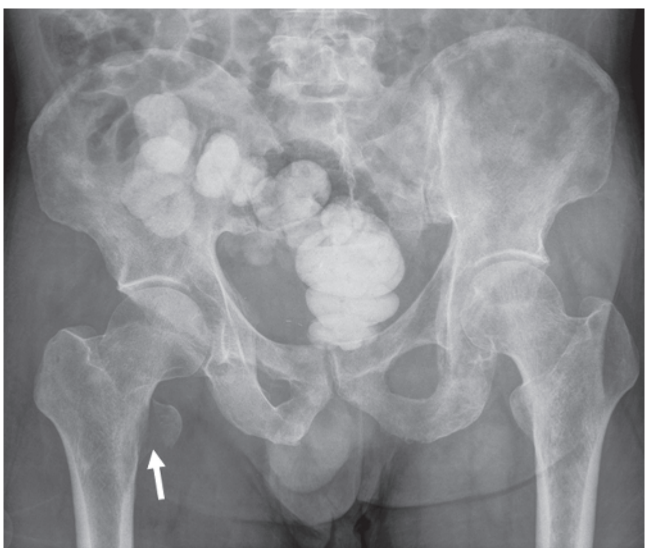

Figure 1.42 Pathologic fracture through the lesser trochanter. AP radiograph of the pelvis shows an avulsion fracture of the right lesser trochanter (arrow). There are mixed lytic and sclerotic osseous lesions in the pelvis and proximal femora bilaterally.

heterotopic ossification may mimic a lytic lesion and soft tissue mass at certain stages of healing. This is especially important in the pelvis with pubic rami and sacral fractures as discussed above (Figure 1.38).

CT is helpful to grade fracture risk in patients with an underlying long bone lytic lesion [58]. Cortical destruction that involves 50% of the cortex is related to increased fracture risk (Figure 1.43) [59]. These patients will undergo prophylactic fixation of the long bone to prevent development of a displaced pathologic fracture. The role of MR to predict fracture risk for pathologic lesions is currently not well understood.

Essential elements of the radiology report

After careful inspection of the radiographs, relevant information should be included in an organized, clear and succinct radiology report. There is a trend toward structured radiology reporting with a recent Radiological Society of North America (RSNA) initiative (http: //www.radreport.org). There are many templates available for MR joint reports.

A negative radiograph study should at minimum state that there is no fracture or malalignment, rather than simply stating "normal". In cases where a fracture is present, it should be accurately described using terminology discussed above. Associated soft tissue and articular findings should be included in the report.

There are numerous classifications systems for fractures. It is important to be familiar with general principles of what features increase the severity of an injury, and potentially influence treatment and outcome. In general, fracture classifications should not be included in the radiology report, as their use may result in miscommunication.

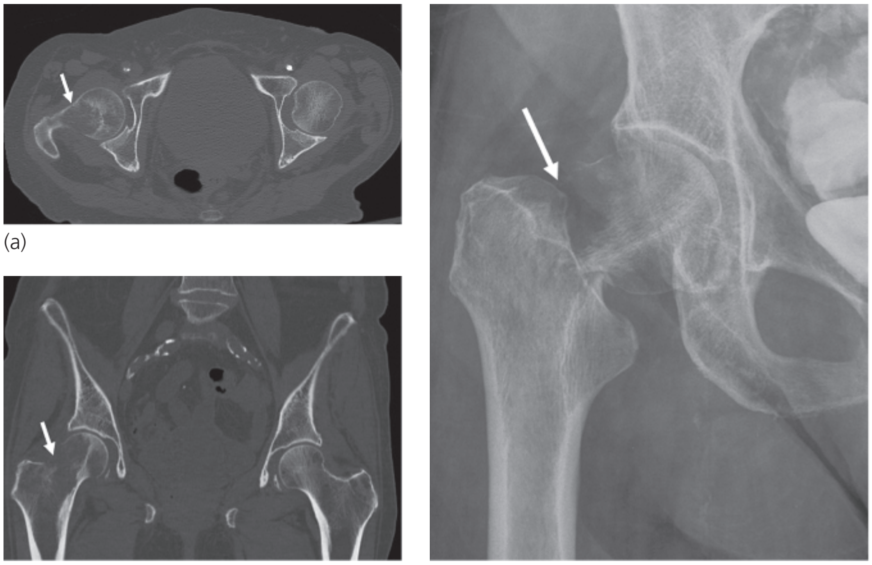

(a) (b) (c)

Figure 1.43 CT for assessment of pathologic fracture risk. (a) Axial and (b) coronal reformatted images show a large lytic lesion in the right femoral head and neck (arrow) with cortical destruction laterally and posteriorly. (c) Two weeks later, radiograph shows a displaced subcapital pathologic fracture (arrow) impacted in varus.

It is preferred that the radiologist accurately describes the fracture, including pertinent findings that may change fracture grade, but not classify a fracture. There is large interobserver variation in the application of fracture classifications to make these systems in radiology reports reliable in all cases [41, 60–62]. Eponyms may lead to further confusion and are best not included in the report.

Many eponyms are defined in the subsequent chapters (ex. Bennett fracture, Jones fracture, Monteggia fracture). Although it is helpful to understand the terminology of eponyms when one communicates with other physicians, their use in radiology reports may lead to confusion since they may not have the same meaning to all users. It is recommended to avoid use of eponyms, and instead, accurately describe a fracture.

At each anatomic site, there are specific statements that are expected to be present. These are included in the chapters that follow for each joint. For example, for distal radial fractures, the report should include whether the fracture is intra-articular, whether there is impaction at the fracture site, angulation of the distal radial articular surface, ulna variance and associated ulnar styoid fractures.

CHECKLIST Statements to be included in all musculoskeletal trauma reports when applicable

- Fracture location (name of bone, location in bone).
- Displacement in terms of shaft width (one half, one full shaft width) and direction of the distal fracture fragment (anterior/posterior, dorsal/volar, dorsal/plantar, medial/lateral).
- Angulation with respect to distal fragment (anterior, posterior, varus, valgus).
- Rotation at the fracture site by assessing the orientation of the joint distal to the fracture.
- Intra-articular extension, and if present, articular gap, depression, step-off deformity, and lipohemarthrosis.
- Alignment at adjacent joints above and below the fracture site (subluxation or dislocation).
- Associated fractures in addition to the main fracture.
- Presence of a skin defect, soft tissue gas, and foreign body.
- Recommendation for additional imaging (additional views, advanced imaging with CT or MR).

References

1 Donaldson LJ, Cook A, Thomson RG. Incidence of fractures in a geographically defined population. *J Epidemiol Community Health*. Sep 1990; **44**(3): 241–245.
2 Kramhoft M, Bodtker S. Epidemiology of distal forearm fractures in Danish children. *Acta Orthop Scand*. Oct 1988; **59**(5): 557–559.
3 Sanders KM, Seeman E, Ugoni AM, *et al*. Age- and gender-specific rate of fractures in Australia: a population-based study. *Osteoporos Int*. 1999; **10**(3): 240–247.
4 Nevitt MC, Cummings SR. Type of fall and risk of hip and wrist fractures: the study of osteoporotic fractures. The Study of Osteoporotic Fractures Research Group. *J Am Geriatr Soc*. Nov 1993; **41**(11): 1226–1234.
5 Rogers LF (ed.). *Radiology of Skeletal Trauma* (3rd edn.). Churchill Livingstone, 2002.
6 Payne SR, Waller JA, Skelly JM, Gamelli RL. Injuries during woodworking, home repairs, and construction. *J Trauma*. Mar 1990; **30**(3): 276–280.
7 Currey JD. The mechanical properties of bone. *Clin Orthop Relat Res*. Nov–Dec 1970; **73**: 209–231.
8 Stiell IG, Greenberg GH, McKnight RD, *et al*. Decision rules for the use of radiography in acute ankle injuries. Refinement and prospective validation. *JAMA*. Mar 3 1993; **269**(9): 1127–1132.
9 Stiell IG, Greenberg GH, Wells GA, *et al*. Prospective validation of a decision rule for the use of radiography in acute knee injuries. *JAMA*. Feb 28 1996; **275**(8): 611–615.

10 Stiell IG, Wells GA, Vandemheen KL, *et al*. The Canadian C-spine rule for radiography in alert and stable trauma patients. *JAMA*. Oct 17 2001; **286**(15): 1841–1848.
11 Lee SI, Chew FS. 1998 ARRS Executive Council Award. Radiology in the emergency department: technique for quantitative description of use and results. American Roentgen Ray Society. *Am J Roentgenol*. Sep 1998; **171**(3): 559–564.
12 Hughston JC. Acute knee injuries in athletes. *Clin Orthop*. 1962; **23**: 114–133.
13 Harley JD, Mack LA, Winquist RA. CT of acetabular fractures: comparison with conventional radiography. *Am J Roentgenol*. Mar 1982; **138**(3): 413–417.
14 Deutsch AL, Mink JH, Waxman AD. Occult fractures of the proximal femur: MR imaging. *Radiology*. Jan 1989; **170**(1 Pt 1): 113–116.
15 Mink JH, Deutsch AL. Occult cartilage and bone injuries of the knee: detection, classification, and assessment with MR imaging. *Radiology*. Mar 1989; **170**(3 Pt 1): 823–829.
16 Elias I, Zoga AC, Morrison WB, *et al*. Osteochondral lesions of the talus: localization and morphologic data from 424 patients using a novel anatomical grid scheme. *Foot Ankle Int*. Feb 2007; **28**(2): 154–161.
17 Linklater JM. Imaging of talar dome chondral and osteochondral lesions. *Top Magn Reson Imaging*. Feb 2010; **21**(1): 3–13.
18 Batillas J, Vasilas A, Pizzi WF, Gokcebay T. Bone scanning in the detection of occult fractures. *J Trauma*. Jul 1981; **21**(7): 564–569.
19 Rosenthall L, Hill RO, Chuang S. Observation of the use of 99mTc-phosphate imaging in peripheral bone trauma. *Radiology*. Jun 1976; **119**(3): 637.
20 Matin P. The appearance of bone scans following fractures, including immediate and long-term studies. *J Nucl Med*. Dec 1979; **20**(12): 1227–1231.
21 Slavin JD, Jr., Mathews J, Spencer RP. Bone imaging in the diagnosis of fractures of the femur and pelvis in the sixth to tenth decades. *Clin Nucl Med*. May 1986; **11**(5): 328–330.
22 Geslien GE, Thrall JH, Espinosa JL, Older RA. Early detection of stress fractures using 99mTc-polyphosphate. *Radiology*. Dec 1976; **121**(3 Pt. 1): 683–687.
23 Hartgerink P, Fessell DP, Jacobson JA, van Holsbeeck MT. Full- versus partial-thickness Achilles tendon tears: sonographic accuracy and characterization in 26 cases with surgical correlation. *Radiology*. Aug 2001; **220**(2): 406–412.
24 Jacobson JA, Lancaster S, Prasad A, *et al*. Full-thickness and partial-thickness supraspinatus tendon tears: value of US signs in diagnosis. *Radiology*. Jan 2004; **230**(1): 234–242.
25 Blab E, Geissler W, Rokitansky A. Sonographic management of infantile clavicular fractures. *Pediatr Surg Int*. 1999; **15**(3–4): 251–254.
26 Eaglesham DC. Visual illusions affecting radiographic interpretation. *J Can Assoc Radiol*. Jun 1968; **19**(2): 96–103.
27 Hall FM. Clinical history, radiographic reporting, and defensive radiologic practice. *Radiology*. Feb 1989; **170**(2): 575–576.
28 Ly JQ, Bui-Mansfield LT. Anatomy of and abnormalities associated with Kager's fat Pad. *Am J Roentgenol.* Jan 2004; **182**(1): 147–154.
29 Olerud S, Karlstrom G, Danckwardt-Lilliestrom G. Treatment of open fractures of the tibia and ankle. *Clin Orthop Relat Res*. Oct 1978(136): 212–224.
30 Gustilo RB, Simpson L, Nixon R, *et al*. Analysis of 511 open fractures. *Clin Orthop Relat Res*. Sep-Oct 1969; **66**: 148–154.
31 Bohndorf K. Injuries at the articulating surfaces of bone (chondral, osteochondral, subchondral fractures and osteochondrosis dissecans). *Eur J Radiol.* Mar 1996; **22**(1): 22–29.
32 Chen CE, Wang JW. Floating knee with ipsilateral knee dislocation: case report. *J Trauma.* Apr 1998; **44**(4): 735–737.
33 Naimark A, Kossoff J, Leach RE. The disparate diameter. A sign of rotational deformity in fractures. *J Can Assoc Radiol*. Mar 1983; **34**(1): 8–11.
34 Tehranzadeh J. The spectrum of avulsion and avulsion-like injuries of the musculoskeletal system. *Radiographics.* Sep 1987; **7**(5): 945–974.
35 Collins DN, Temple SD. Open joint injuries. Classification and treatment. *Clin Orthop Relat Res*. Jun 1989(243): 48–56.
36 Fracture and dislocation compendium. Orthopaedic Trauma Association Committee for Coding and Classification. *J Orthop Trauma*. 1996; **10** Suppl 1: v-ix, 1–154.
37 Matheson GO, Clement DB, McKenzie DC, Taunton JE, Lloyd-Smith DR, MacIntyre JG. Stress fractures in athletes. A study of 320 cases. *Am J Sports Med*. Jan–Feb 1987; **15**(1): 46–58.
38 Schneider HJ, King AY, Bronson JL, Miller EH. Stress injuries and developmental change of lower extremities in ballet dancers. *Radiology.* Dec 1974; **113**(3): 627–632.
39 Chamay A. Mechanical and morphological aspects of experimental overload and fatigue in bone. *J Biomech.* May 1970; **3**(3): 263–270.
40 Fowler JR, Gaughan JP, Boden BP, Pavlov H, Torg JS. The non-surgical and surgical treatment of tarsal navicular stress fractures. *Sports Med*. Aug 1 2011; **41**(8): 613–619.
41 Ting A, King W, Yocum L, *et al*. Stress fractures of the tarsal navicular in long-distance runners. *Clin Sports Med.* Jan 1988; **7**(1): 89–101.
42 Daffner RH, Pavlov H. Stress fractures: current concepts. *Am J Roentgenol.* Aug 1992; **159**(2): 245–252.
43 Boden BP, Speer KP. Femoral stress fractures. *Clin Sports Med.* Apr 1997; **16**(2): 307–317.
44 Boden BP, Osbahr DC. High-risk stress fractures: evaluation and treatment. *J Am Acad Orthop Surg*. Nov–Dec 2000; **8**(6): 344–353.
45 Boden BP, Osbahr DC, Jimenez C. Low-risk stress fractures. *Am J Sports Med*. Jan–Feb 2001; **29**(1): 100–111.
46 Greaney RB, Gerber FH, Laughlin RL, *et al*. Distribution and natural history of stress fractures in U.S. Marine recruits. *Radiology*. Feb 1983; **146**(2): 339–346.
47 Lee JK, Yao L. Stress fractures: MR imaging. *Radiology.* Oct 1988; **169**(1): 217–220.
48 Prather JL, Nusynowitz ML, Snowdy HA, *et al*. Scintigraphic findings in stress fractures. *J Bone Joint Surg Am.* Oct 1977; **59**(7): 869–874.
49 Murcia M, Brennan RE, Edeiken J. Computed tomography of stress fracture. *Skeletal Radiol.* 1982; **8**(3): 193–195.
50 Lenart BA, Lorich DG, Lane JM. Atypical fractures of the femoral diaphysis in postmenopausal women taking alendronate. *N Engl J Med*. Mar 20 2008; **358**(12): 1304–1306.
51 Schneider R, Kaye JJ. Insufficiency and stress fractures of the long bones occurring in patients with rheumatoid arthritis. *Radiology.* Sep 1975; **116**(3): 595–599.
52 Donovan A, Schweitzer ME, Rafii M, Lax A. Radiological features of superomedial iliac insufficiency fractures: a possible mimicker of metastatic disease. *Skeletal Radiol.* Jan 2009; **38**(1): 43–49.
53 Jung HS, Jee WH, McCauley TR, *et al*. Discrimination of metastatic from acute osteoporotic compression spinal fractures with MR imaging. *Radiographics*. Jan–Feb 2003; **23**(1): 179–187.
54 Erly WK, Oh ES, Outwater EK. The utility of in-phase/opposed-phase imaging in differentiating malignancy from acute benign compression fractures of the spine. *AJNR Am J Neuroradiol*. Jun–Jul 2006; **27**(6): 1183–1188.
55 Campbell SE, Fajardo RS. Imaging of stress injuries of the pelvis. *Semin Musculoskelet Radiol.* Mar 2008; **12**(1): 62–71.
56 Krishnamurthy GT, Tubis M, Hiss J, Blahd WH. Distribution pattern of metastatic bone disease. A need for total body skeletal image. *JAMA*. Jun 6 1977; **237**(23): 2504–2506.
57 Habermann ET, Sachs R, Stern RE, *et al*. The pathology and treatment of metastatic disease of the femur. *Clin Orthop Relat Res.* Sep 1982(169): 70–82.
58 Keene JS, Sellinger DS, McBeath AA, Engber WD. Metastatic breast cancer in the femur. A search for the lesion at risk of fracture. *Clin Orthop Relat Res.* Feb 1986(203): 282–288.

59 Hipp JA, Springfield DS, Hayes WC. Predicting pathologic fracture risk in the management of metastatic bone defects. *Clin Orthop Relat Res*. Mar 1995(312): 120–135.

60 Andersen DJ, Blair WF, Steyers CM Jr., *et al*. Classification of distal radius fractures: an analysis of interobserver reliability and intraobserver reproducibility. *J Hand Surg Am.* Jul 1996; **21**(4): 574–582.

61 Andersen E, Jorgensen LG, Hededam LT. Evans' classification of trochanteric fractures: an assessment of the interobserver and intraobserver reliability. *Injury.* Nov 1990; **21**(6): 377–378.

62 Dirschl DR, Adams GL. A critical assessment of factors influencing reliability in the classification of fractures, using fractures of the tibial plafond as a model. *J Orthop Trauma.* Oct 1997; **11**(7): 471–476.